ECT* EUROPEAN CENTRE FOR THEORETICAL STUDIES IN NUCLEAR PHYSICS AND RELATED AREAS
FONDAZIONE BRUNO KESSLER
Theoretical Motivations and Empirical Evidence for Diquark Correlations in Hadrons

Tetraquarks in lattice QCD

Ying Chen

Institute of High Energy Physics, Chinese Academy of Sciences, China

Oct. 20, 2026, ECT*, Trento, Italy

Outline

I. Introduction

II. $T_{cc}^{+}(3875)$ and $X(3872)$ on the lattice

III. T_{bb} ——Counterpart of $T_{cc}^{+}(3875)$

IV. Fully charm tetraquark systems in di-charmonium scatterings

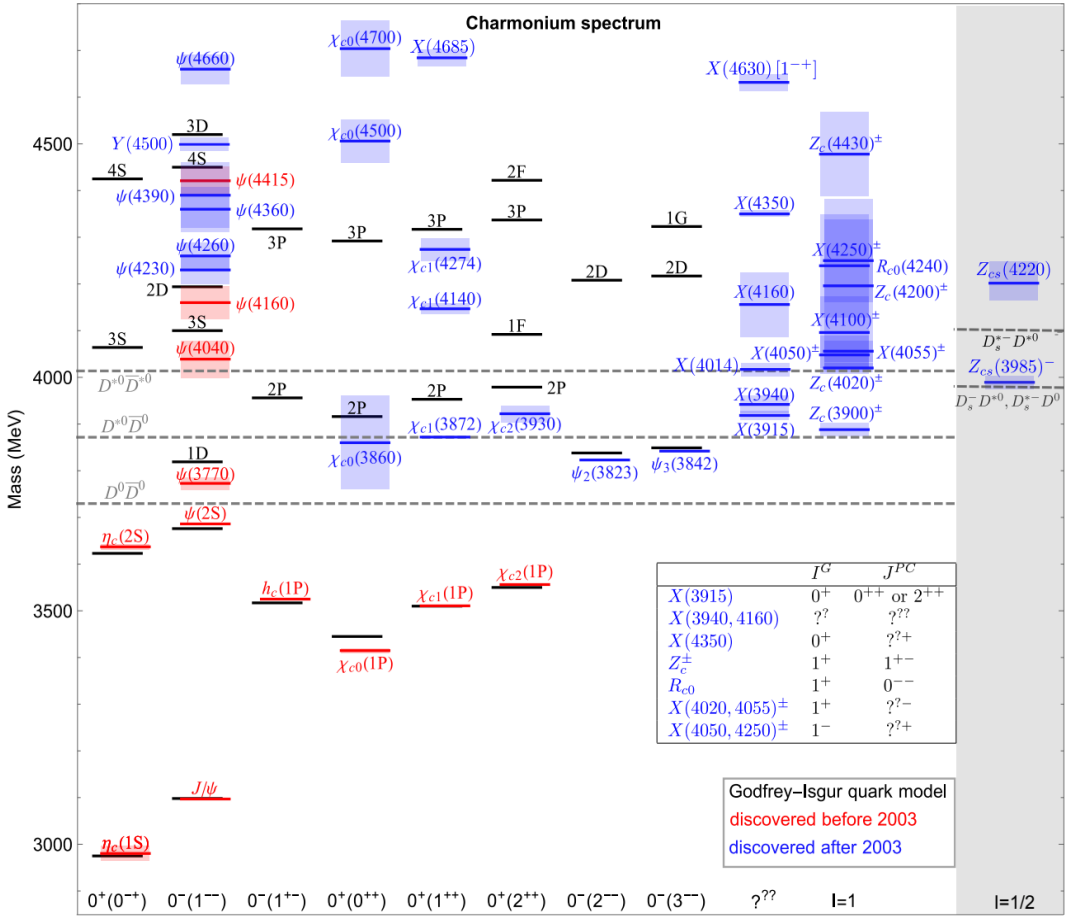
V. Discussion on the relevance (or not) of local tetraquark operators

VI. Summary

I. Introduction

1. Tetraquark systems——Four-quark-states as the minimum configuration

- Ever since the discovery of X(3872), a large number of charmium(-like) structures have been observed by various experiments (BESIII, BaBar, Belle, CDF, D0, ATLAS, CMS and LHCb).
- All of the XYZ states are above or at least in the vicinity of the open-charm thresholds, and are good candidates for hadron molecules.
- In 2021, LHCb observed the first doubly charmed structure $T_{cc}^{+}(3875)$.
- Fully charm tetraquark systems in $J/\psi J/\psi$ spectrum
  $X(6600), X(6900), X(7200)$
- Their properties are worthy of a investigation in depth.
- Lattice QCD plays an important role through
  Hadron-hadron scatterings
- Recently, arguments emerge on the necessary of the inclusion of tetraquark operators.



2. Theoretical interpretation of tetraquark states

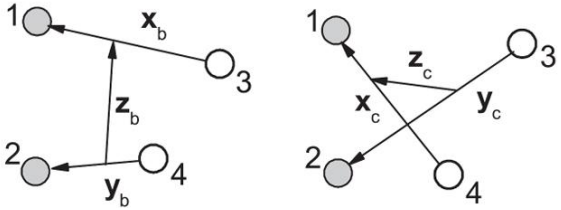
- Hadron molecule: $(H_1H_2)(J^{P(C)})$, hadron-hadron interaction through meson exchanges

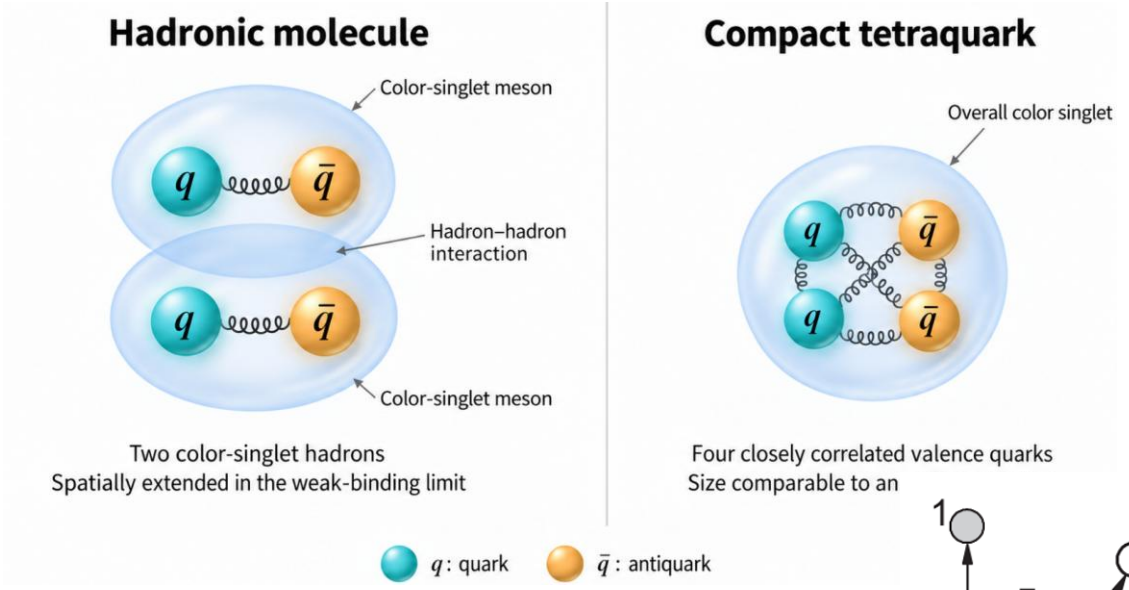
  $X(3872)\leftrightarrow D^0\bar{D}^{*0}(L=0,I=0),\ J^{PC}=1^{++}$

  $T_{cc}^{+}(3875)\leftrightarrow DD^{*}\ (L=0,I=0),\ J^{P}=1^{+}$

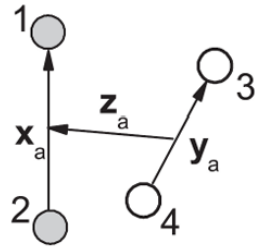
  $Z_c^{+}(3900)\leftrightarrow D\bar{D}^{*}\ (L=0,I=1),\ J^{P}=1^{+}$

  ……





- Compact tetraquark: $[q_1q_2]^i[\bar{q}_3\bar{q}_4]_i\ (J^{P(C)})$, bound states made up of diquark-anti-diquark pair



$[q_1q_2]_S^{C,F}(J^P,I)$:

$\Psi=\Phi_{flavor}\otimes\Phi_{color}\otimes\Phi_{spin}\otimes\Phi_{space}$

Φ_{flavor}: depends on q_1,q_2 (S, A)

$\Phi_{color}(C)$: $\underline{3^*}$ (attractive one-gluon-exchange)

$\Phi_{spin}(S)$: $S=0,1$

Φ_{space}: $l=0$

$X(3872)\leftrightarrow[cu]_0^{3^*,A}\,[\bar{c}\bar{u}]_1^{3,S}(L=0,I=0),$

$T_{cc}^{+}(3875)\leftrightarrow[cc]_1^{3^*,S}[\bar{u}\bar{d}]_0^{3,A}\ (L=0,I=0),$

$Z_c^{+}(3900)\leftrightarrow[cu]_0^{3^*,A}[\bar{c}\bar{d}]_1^{3,S}(L=0,I=1)$

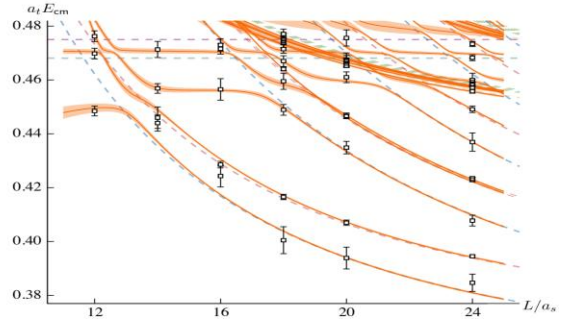
$X(6600)\leftrightarrow[cc]_1^{3^*,S}[\bar{c}\bar{c}]_1^{3,S}\ (L=0),\ J^{PC}=(0,2)^{++}$

3. The methodology for studying hadron-hadron scattering in lattice QCD

State-of-art Approach——Lellouch-Lüscher's formalism

(see R. Briceno et al., Rev. Mod. Phys. 90 (2018) 025001 for a review).

$$\det\left[F^{-1}\left(\vec{P},E,L\right)+\mathcal{M}(E)\right]=0$$



$E_n(L)$: Eigen-energies of lattice Hamiltonian.

- **Interpolation field operator set** for a given J^{PC}

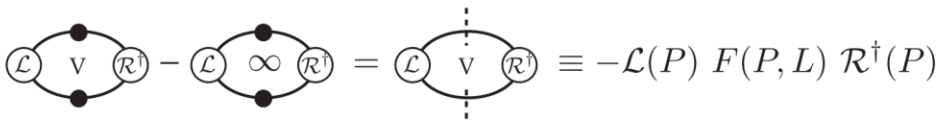
  $\mathcal{O}_i$: $\bar{q}_1\Gamma q_2$ $[\bar{q}_1\Gamma_1 q][\bar{q}\Gamma_2 q_2]$ $[q_1^T\Gamma_1 q][\bar{q}\Gamma_2\bar{q}_2^T]$, …
- **Correlation function matrix** —— **Observables**

$$C_{ij}(t)\& = \left\langle\Omega\middle|\mathcal{O}_i(t)\mathcal{O}_j^+(0)\middle|\Omega\right\rangle$$

$$=\sum_n\langle\Omega|\mathcal{O}_i|n\rangle\left\langle n\middle|\mathcal{O}_j^+\middle|\Omega\right\rangle e^{-E_n t}$$

All the energy levels $E_n(L)$ are discretized.

$F\left(\vec{P},E,L\right)$: Mathematically known function matrix in the channel space (the explicit expression omitted

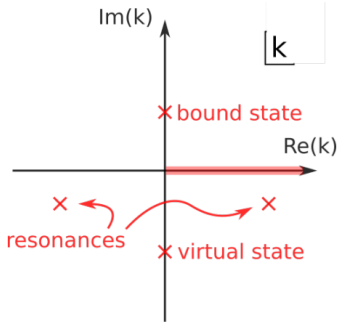


$\mathcal{M}(E)$: Scattering matrix.

- Unitarity requires

$$\mathcal{M}_{ab}^{-1}=(\mathcal{K}^{-1})_{ab}-i\delta_{ab}\frac{2q_a^*}{E_{cm}}$$

- $\mathcal{K}$ is a real function of s for real energies above kinematic threshold.
- The pole singularities of $\mathcal{M}(s)$ in the complex s-plane correspond to bound states, virtual states, resonances, etc..

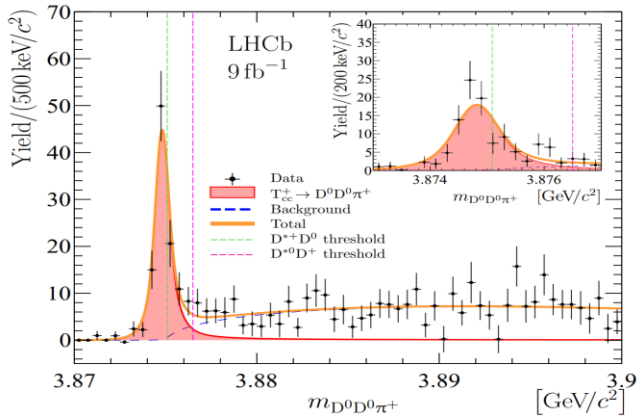


$$k=\pm\frac{1}{2}\sqrt{s-4m^2}$$

II. $T_{cc}^{+}(3875)$ and $X(3872)$ on the lattice

1. Lattice studies of $T_{cc}^{+}(3875)$

LHCb discovered $T_{cc}^{+}(3875)$ in 2021 (LHCb, Nature Phys.18, 751 (2022), Nature Comm.13, 3551 (2022))



$$M_{T_{cc}} - \left(m_{D^0} + m_{D^{*+}}\right) = -273 \pm 61 \pm 5^{+11}_{-14}\ \text{keV}$$

$$\Gamma_{BW} = 410 \pm 165 \pm 43^{+18}_{-38}\ \text{keV}$$

$$\Gamma^{U}_{BW} = 48 \pm 2^{0}_{-14}\ keV$$

Isospin：Only observed in DD^{*+}, therefore $I = 0$

The minimum quark configuration：$cc\bar{u}\bar{d}$

- Spured extensive and intensive phemonenological investigations
- Likely a DD^* hadronic molecule
- A relay race of lattice studies——make the things clearer!

Pole singularity:	M. Padmanath and S. Prelovsek, Phys. Rev. Lett. 129 (2022) 032002
Dynamics underlying:	S. Chen et al., Phys. Lett. B 833, 137391 (2022)
Interaction potential:	Y. Lyu et al., Phys. Rev. Lett. 131, 161901 (2023)
$DD^* - D^*D^*$ coupled channels:	T. Whyte et al.(HSC), Phys. Rev. D 111, 034511 (2025)
DD^* and T_{4q} operators:	Prelovsek et al., Phys. Rev. D 112, 014507 (2025)

A. Pole singularity of $DD^*(I=0)$ from lattice QCD

DD^* operators only

(M. Padmanath and S. Prelovsek, Phys. Rev. Lett. 129 (2022) 032002)

$$e^{2i\delta_l} = 1 + i\,2\rho t_l, \rho = \frac{2p}{\sqrt{s}}, \qquad \sqrt{s} = E_{cm} = \sqrt{m_D^2 + p^2} + \sqrt{m_{D^*}^2 + p^2}$$

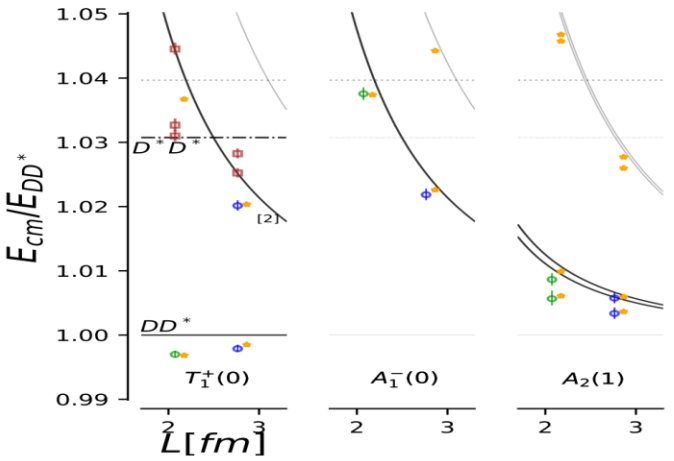
S-wave scattering amplitude: $t_0 = \frac{\sqrt{s}}{2}\frac{1}{p\cot\delta_0 - ip}$

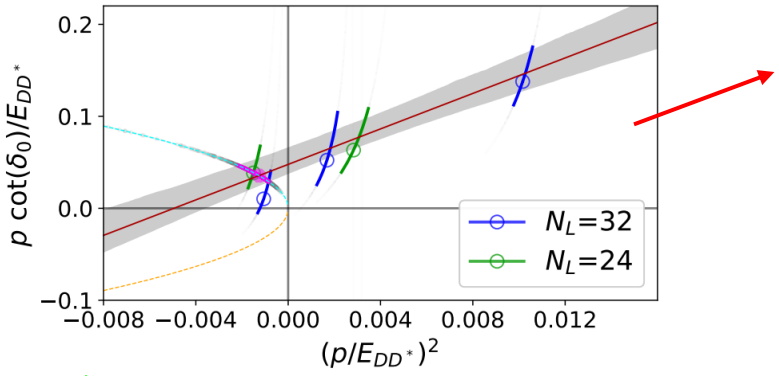
Lüscher's relation:

$$p\cot\delta_0(q^2) = \frac{2}{L\sqrt{\pi}}\mathcal{Z}_{00}(1,q^2) = \frac{1}{\pi L}\sum_{\vec{n}\in Z_3}\frac{1}{\vec{n}^2 - q^2}, q = \frac{Lp}{2\pi}$$

Effective range expansion (ERE): $p\cot\delta_0 = \frac{1}{a_0} + \frac{1}{2}r_0p^2$

ID	$\vec{P}$	LG	Λ^P	J^P	l	interpolators: $M_1(\vec{p}_1^{\,2})M_2(\vec{p}_2^{\,2})$
1	$(0,0,0)$	O_h	T_1^+	1^+	$0,2$	$D(0)D^*(0),\ D(1)D^*(1)\ [2],\ D^*(0)D^*(0)$
2	$(0,0,0)$	O_h	A_1^-	0^-	1	$D(1)D^*(1)$
3	$(0,0,1)\frac{2\pi}{L}$	Dic_4	A_2	$0^-,1^+,2^-$	$0,1,2$	$D(0)D^*(1),\ D(1)D^*(0)$
4	$(1,1,0)\frac{2\pi}{L}$	Dic_2	A_2	$0^-,1^+,2^-,2^+$	$0,1,2$	$D(0)D^*(2),\ D(1)D^*(1)\ [2],\ D(2)D^*(0)$
5	$(0,0,2)\frac{2\pi}{L}$	Dic_4	A_2	$0^-,1^+,2^-$	$0,1,2$	$D(1)D^*(1)$

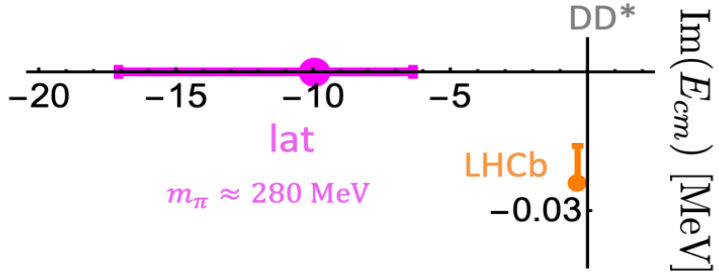




Pole condition: $p\cot\delta_0 = ip$

$$p = \pm i|p|$$
$$ip = \mp\sqrt{|p^2|},$$

$\delta m_{T_{cc}} = \mathrm{Re}(E_{cm}) - m_{D^0} - m_{D^{*+}}$ [MeV]



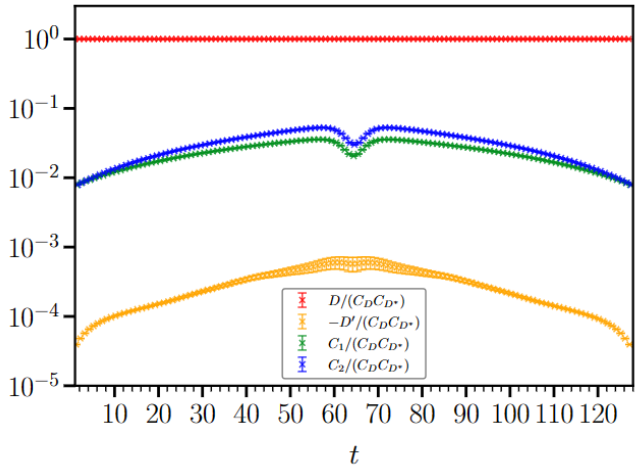
B. Investigation of the isospin-dependent interaction of DD^* scattering

(S. Chen et al., Phys. Lett. B 833, 137391 (2022))

$$p\cot\delta_0(p) = \frac{1}{a_0} + \frac{1}{2}r_0p^2 + \mathcal{O}(p^4)$$

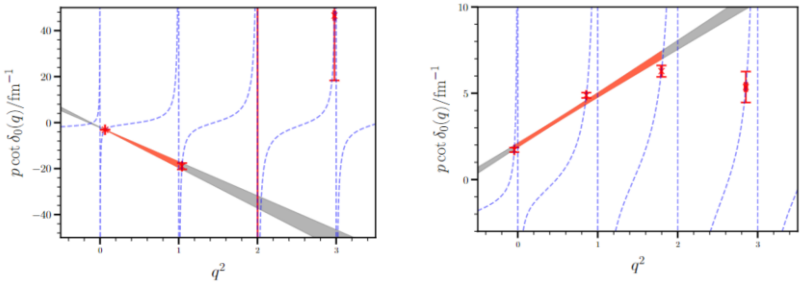
- DD^* energies and scattering momenta can be derived precisely
- Single-channel Lüscher's formula applied
- $I = 1$ DD^* is repulsive, $I = 0$ DD^* is repulsive (sign of a_0)
- Quark diagrams (after Wick's contraction) contributing to DD^* correlators

$$C^{(I)}_{DD^*}(t) = D + C_1 + (-)^{I+1}(C_2 + D')$$

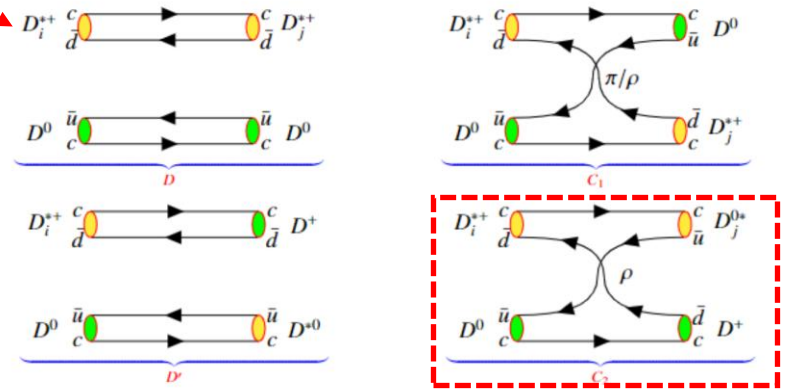


$$\Delta E^{(I)}_{DD^*} \approx \epsilon_1\delta E_1 + (-)^{I+1}\epsilon_2\delta E_2$$
$$(\epsilon_2 > \epsilon_1 > 0, \quad \delta E_2 \geq \delta E_1)$$

$$\begin{cases} \Delta E^{(I=0)}_{DD^*} < 0, \\ \Delta E^{(I=1)}_{DD^*} > 0, \end{cases}$$



$I = 1$: repulsive $I = 0$: attractive



Schematic quark diagrams

- Initiatively interprets the underlying physics by analyzing the quark diagrams in lattice QCD calculations

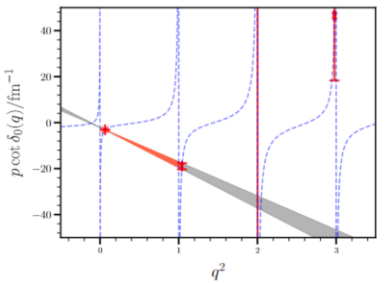
B. Investigation of the isospin-dependent interaction of DD^* scattering

(S. Chen et al., Phys. Lett. B 833, 137391 (2022))

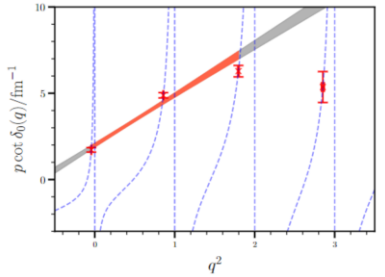
$$p\cot\delta_0(p) = \frac{1}{a_0} + \frac{1}{2}r_0p^2 + \mathcal{O}(p^4)$$

- DD^* energies and scattering momenta can be derived precisely
- Single-channel Lüscher's formula applied
- $I = 1$ DD^* is repulsive, $I = 0$ DD^* is repulsive (sign of a_0)
- Quark diagrams (after Wick's contraction) contributing to DD^* correlators

$$C_{DD^*}^{(I)}(t) = D + C_1 + (-)^{I+1}(C_2 + D')$$



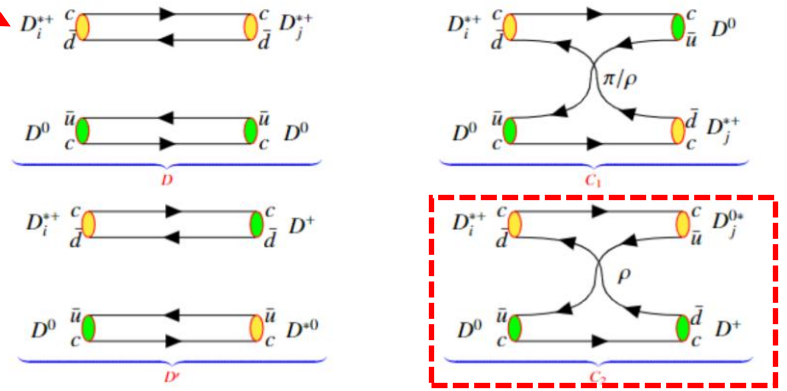
$I = 1$: repulsive



$I = 0$: attractive

- ✓ D' term is negligible.
- ✓ C_2 term is responsible for the energy difference of $DD^*(I = 1)$ and $DD^*(I = 0)$.
- ✓ C_2 term can be understood as the exchange of charged vector ρ meson, which provides attractive (repulsive) interaction for $I = 0$ $(I = 1)$
- ✓ This is in qualitative agreement with phenomenological studies (Dong et al. CTP73 (2021) 125201, Feijoo et al, PRD104(2021)114015)

- Initiatively interprets the underlying physics by analyzing the quark diagrams in lattice QCD calculations



Schematic quark diagrams

C. Hadron-hadron interaction potential——HALQCD approach (Y. Lyu et al., arXiv:2302.04505 (hep-lat))

- (2+1)-flavor QCD on the 96^4 lattice with $m_\pi = 146.4\ \mathrm{MeV}$, L=8.1 fm
- Calculate the correlation functions

Nambu-Bethe-Salpeter wave function

$$R(\vec{r},t) = e^{(m_{D^*}+m_D)t}\sum_{\vec{x}}\langle 0|D^*(\vec{x}+\vec{r},t)D(\vec{x},t)\bar{J}(0)|0\rangle = \sum_n A_n\psi_n(\vec{r})e^{-\Delta E_n t} + \cdots$$

- The function $R(\vec{r},t)$ satisfies the Shrödinger-type equation

$$\left[\frac{1+3\delta^2}{8\mu}\partial_t^2 - \partial_t - H_0 + \cdots\right]R(\vec{r},t) = \int d\vec{r}\,' U(\vec{r},\vec{r}\,')R(\vec{r},t), \qquad H_0 = -\frac{\nabla^2}{2\mu}, \qquad \mu = \frac{m_{D^*}m_D}{m_{D^*}+m_D}, \qquad \delta = \frac{m_{D^*}-m_D}{m_{D^*}+m_D}$$

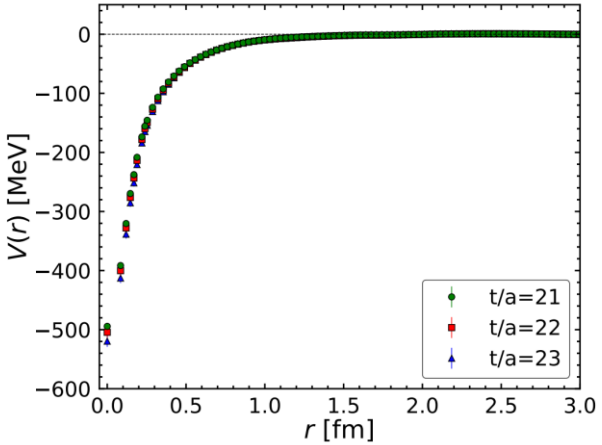
- Takes the leading term of derivative expansion of the non-local $U(\vec{r},\vec{r}\,')$

$$U(\vec{r},\vec{r}\,') \approx V(\vec{r})\delta(\vec{r}-\vec{r}\,'), \qquad V(r) = R^{-1}(\vec{r},t)\left[\frac{1+3\delta^2}{8\mu}\partial_t^2 - \partial_t - H_0 + \cdots\right]R(\vec{r},t)$$

- The DD^* potential in the $(I,J^P) = (0,1^+)$ channel is attractive.
- Short range: attractive diquark-antidiquark $(\bar{u}\bar{d} - cc)$
  Long range: two-pion exchange is favored:

$$V_{fit}^B(r;m_\pi) = \sum_{i=1,2} a_i e^{(-r/b_i)^2} + a_3\left(\frac{1}{r}e^{-m_\pi r}\right)^2 \cdots$$

- Different from phenomenological expectation that ρ-exchange dominates?



C. Hadron-hadron interaction potential——HALQCD approach (Y. Lyu et al., arXiv:2302.04505 (hep-lat))

- Using the derived potential, the S-wave phase shifts δ_0 is obtained by solving the Schrödinger equation of DD^* system, which is put into the ERE

$$p\cot\delta_0(p) = \frac{1}{a_0} + \frac{1}{2}r_0p^2 + \mathcal{O}(p^4)$$

- Extrapolate to the physical m_π,

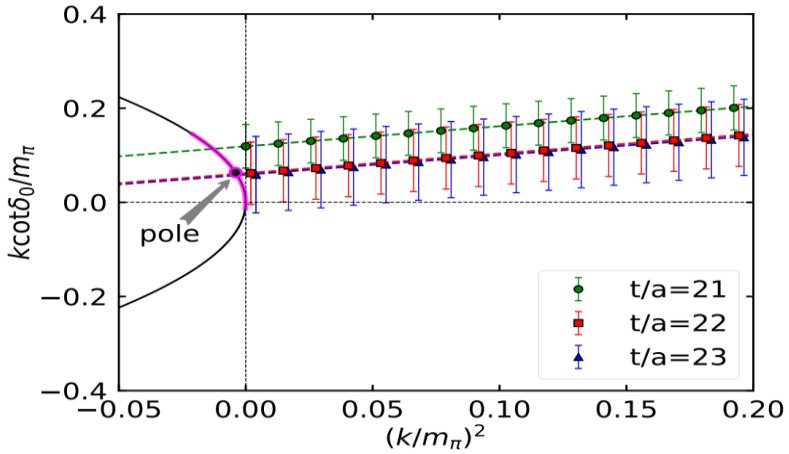
$$V^B_{fit}(r;m_\pi) \to V^B_{fit}\left(r;m_\pi^{\text{phys}}\right)$$

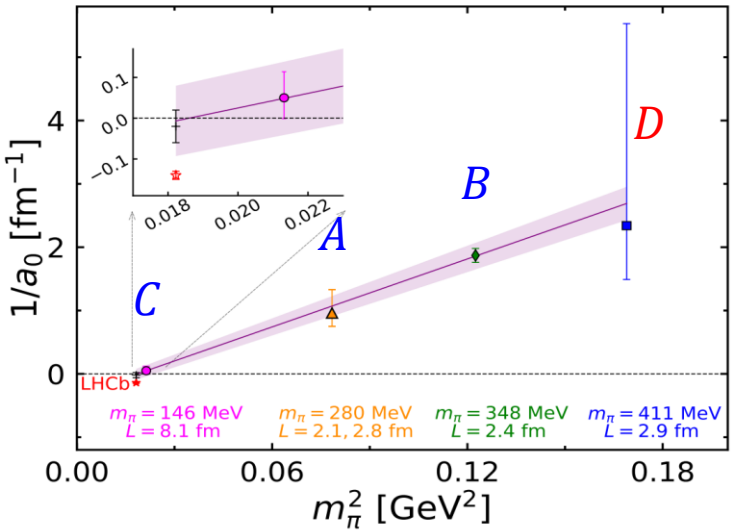
on

m_π [MeV]	146.4	135.0
$1/a_0$ [fm^{-1}]	$0.05(5)\binom{+4}{-1}$	$-0.02(4)$
r_{eff} [fm]	$1.14(6)\binom{+1}{-9}$	$1.14(8)$
κ_{pole} [MeV]	$-9(9)\binom{+1}{-8}$	$+3(8)$
E_{pole} [keV]	$-45(77)\binom{+02}{-99}$	$-10(37)$

consistent with the large negative scattering length a_0 of a bound state ($k = i\kappa_{\text{pole}}$).

- This result is consistent with the extrapolated a_0 using the existing lattice results.



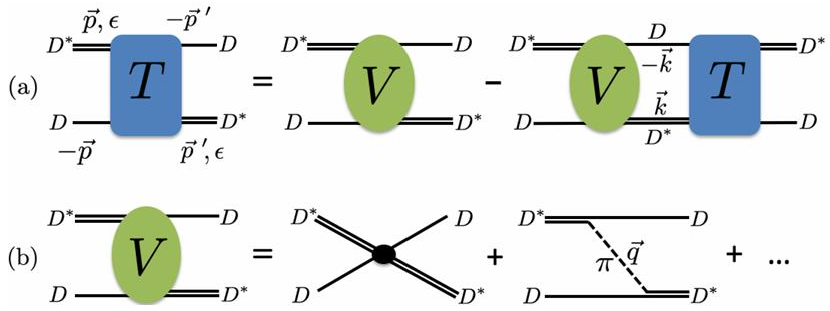


D: Y. Ikeda et al. (HALQCD) Phys. Lett. B 729 (2014) 84-90

D. Left-hand-cut issue owing to pion exchange——changes the pole extraction

M. Du et al., Phys.Rev.Lett. 131 (2023) 13, 131903; Meng et al., Phys. Rev. D 109, L071506 (2024)

- Hadron-hadron interaction and LSE.



$$V(p,p') = V_{CT} + 3\left(\frac{g}{2f_\pi}\right)^2 \frac{(\vec{\epsilon}\cdot\vec{q})(\vec{\epsilon}'^{*}\cdot\vec{q})}{q^2 - m_\pi^2},$$

$$V(r) = V_{CT}\delta(\vec{r}) + 3\left(\frac{g}{2f_\pi}\right)^2\left(-\delta(\vec{r}) + \frac{\mu_\pi^2}{4\pi r}e^{-\mu_\pi r}\right)$$

- Attractive short-range int. vs. Yukawa type long-range repulsive owing to pion exchange. The later can render the virtual state into a resonance

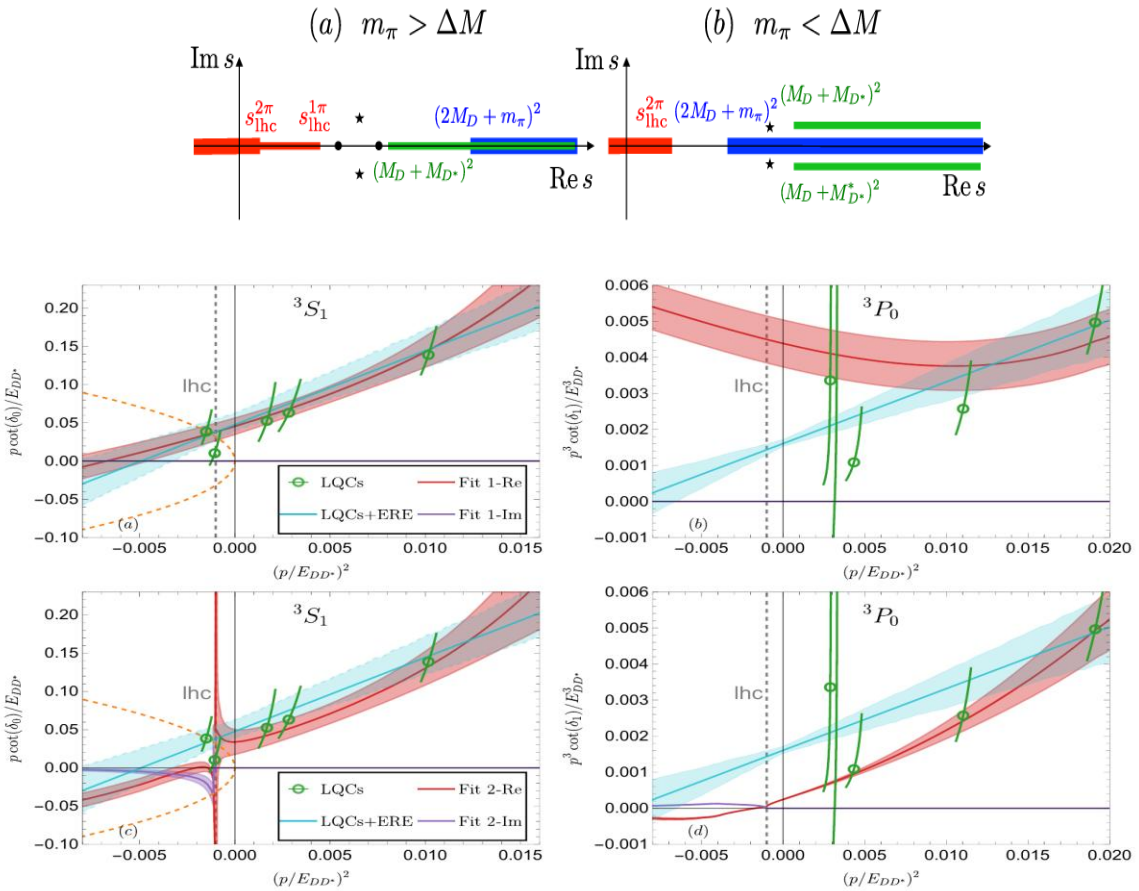


Fig. 3: fits without pion exchange (top) and with pion exchange (bottom)

E. DD^* and T_{4q} operators both considered——seemling relevance of T_{4q}

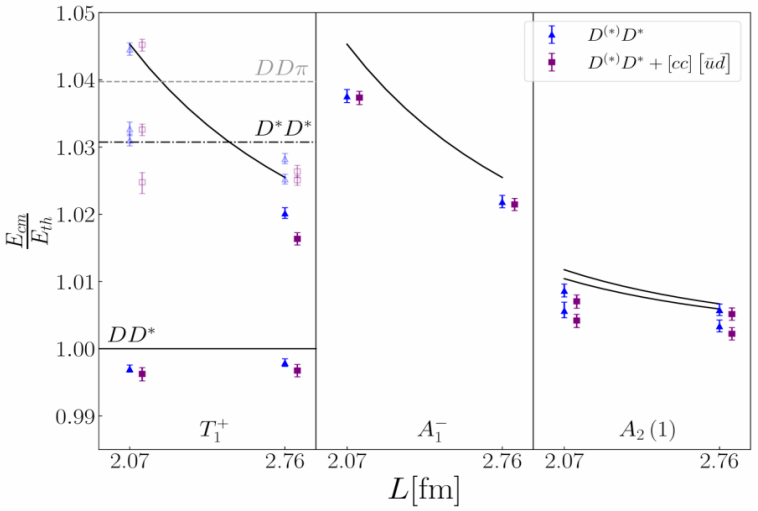
(Prelovsek et al., Phys. Rev. D 112, 014507 (2025))

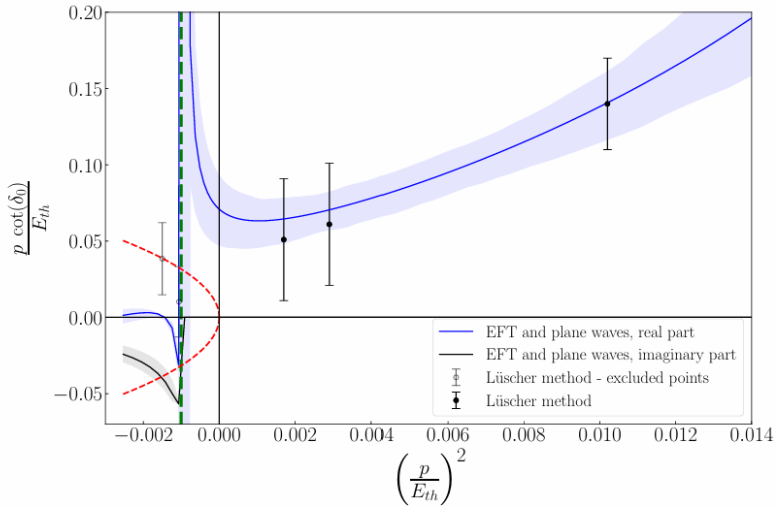
- Both local diquark–antidiquark operators and meson-meson operators are involved.

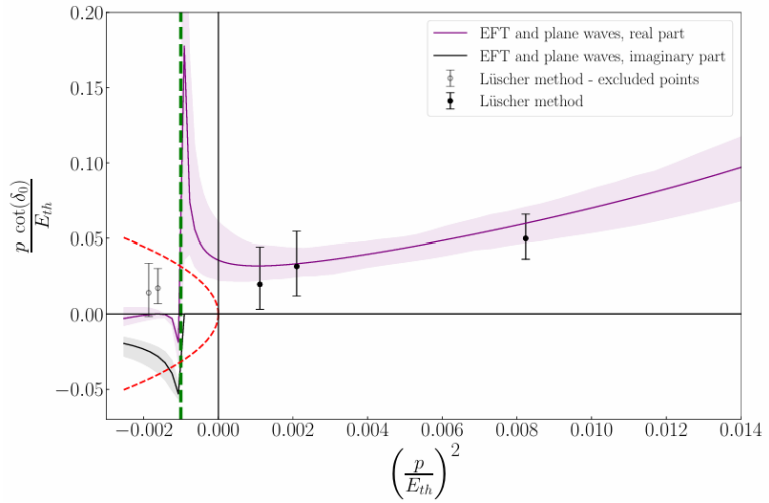
$$\mathcal{O}^{4q} = [cc]_1^{3^*,S}\left[\bar{u}\bar{d}\right]_0^{3,A}$$

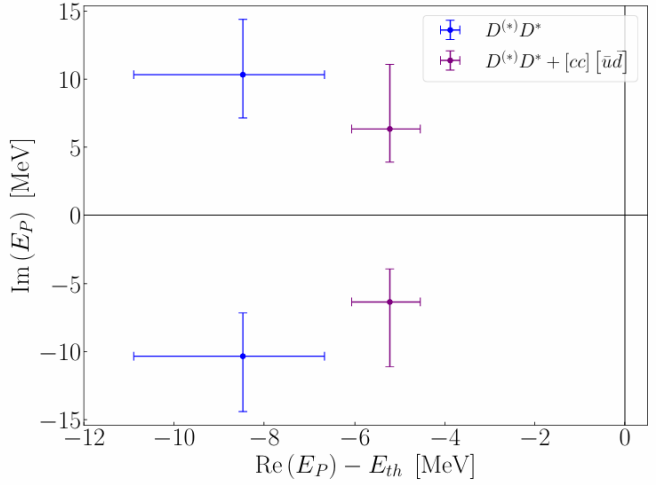
- The inclusion of $\mathcal{O}^{4q}$ shifts energy levels a little.
- EFT(OPE) analysis obtains a sub-threshold resonance pole at $m_\pi = 280$ MeV.
- A recent study (without $\boldsymbol{\mathcal{O}^{4q}}$) (A.P. Lachini and R.A Briceno, 2607.19009) obtains the similar result ($m_\pi = 391$ MeV).

$D^{(*)}D^*$ FVE w/o $\mathcal{O}^{4q}$ (purple/blue)





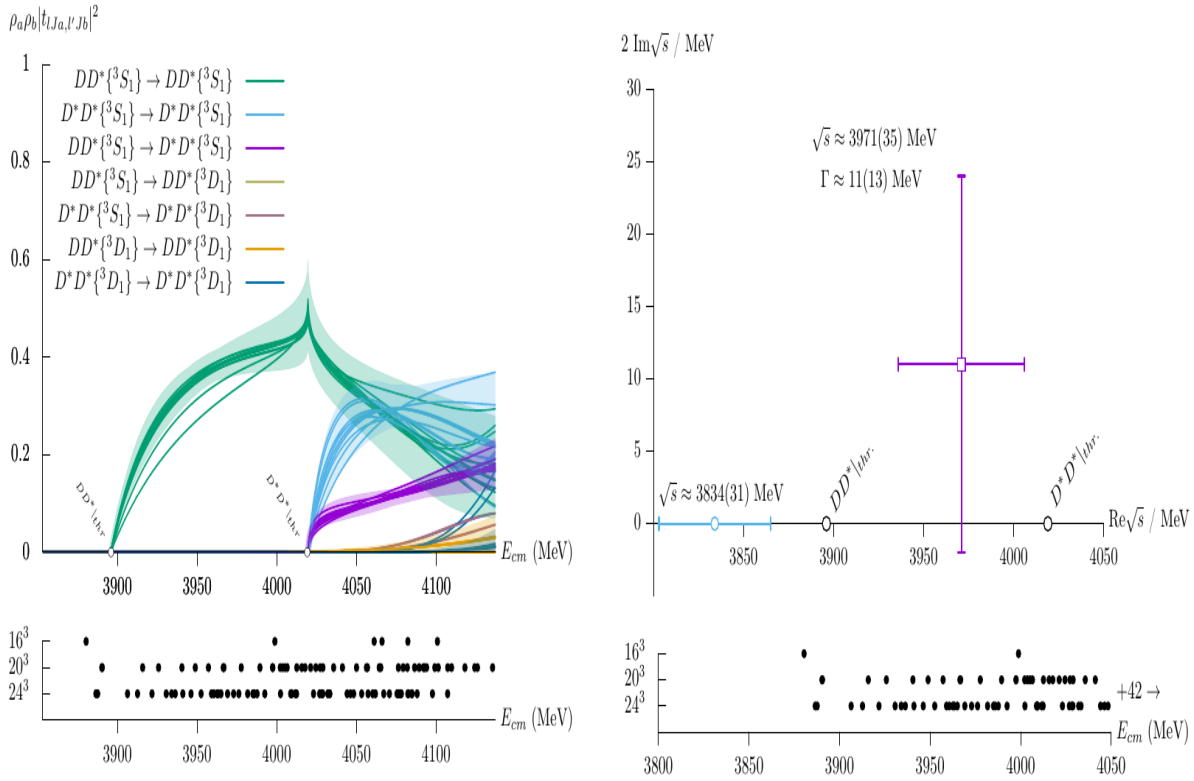




F. $DD^* - D^*D^*$ coupled channels——a virtual pole below DD^* threshold and a T_{cc}'

(Whyte, Wilson & Thomas, Phys. Rev. D 111, 034511 (2025))

- Coupled DD* and D*D* scattering for $I(J^P) = 0(1^+)$ at $m_\pi = 391$ MeV.
- Analytic continuation yields a virtual pole below DD* threshold and a second pole below D*D* threshold.
- The upper pole remains a resonance because the lower channel is open.
- Interchannel coupling produces a cusp at the upper threshold.
- The higher pole couples strongly to D*D*. Its location is specific to the simulated pion mass.
- The result motivates a partner-state search, while its physical-mass pole pattern requires additional quark-mass and three-body studies.



Coupled amplitudes, pole positions and constraining energy levels

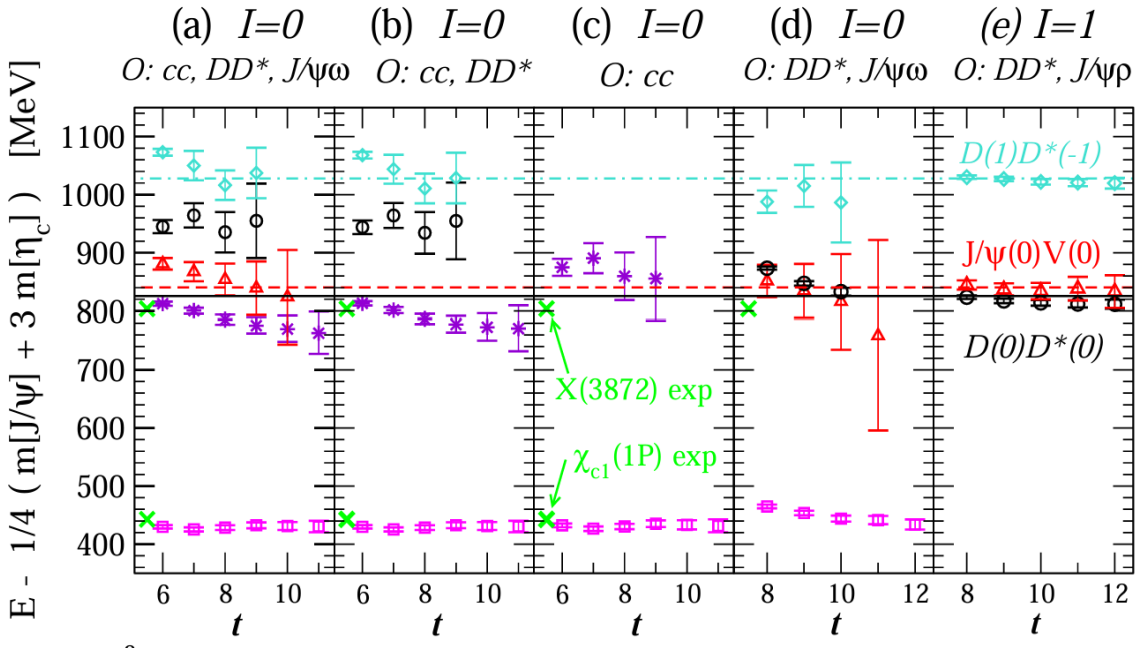
2. Lattice studies of $X(3872)$

- **X(3872) found in 2003 by Belle, quite a lot of XYZ particles observed afterwards**

$$m_X = 3871.65 \pm 0.06\ \text{MeV}$$
$$\Gamma_X = 1.19 \pm 0.21\ \text{MeV}$$
$$I^G J^{PC} = 0^+ 1^{++}$$

- **X(3872) decays mainly to $D^0 \bar{D}^{0*}$, a small fraction to $J/\psi\omega$, and also isospin violating $J/\psi\rho$**
- **Intensive and extensive phenomenological studies**
- **Interpreted as a $c\bar{c}$, a $D\bar{D}^*$ molecule or a tetraquark**
- **Main point of view: $D\bar{D}^* + c\bar{c}$**

S. Prelovsek et al. Phys.Rev.Lett. 111 (2013) 192001

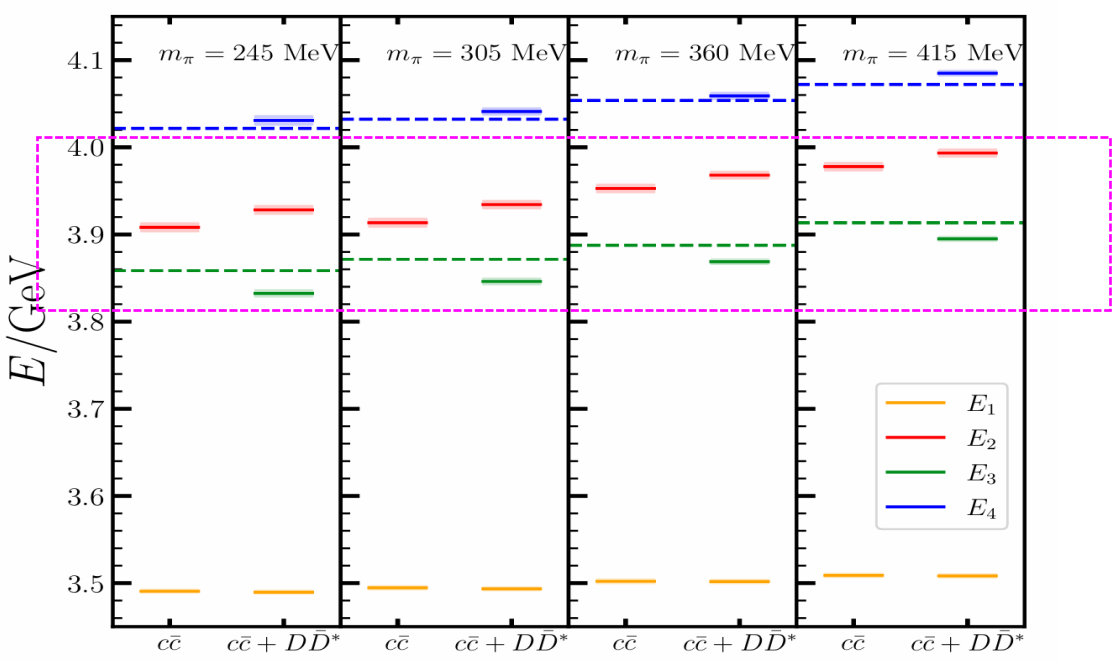


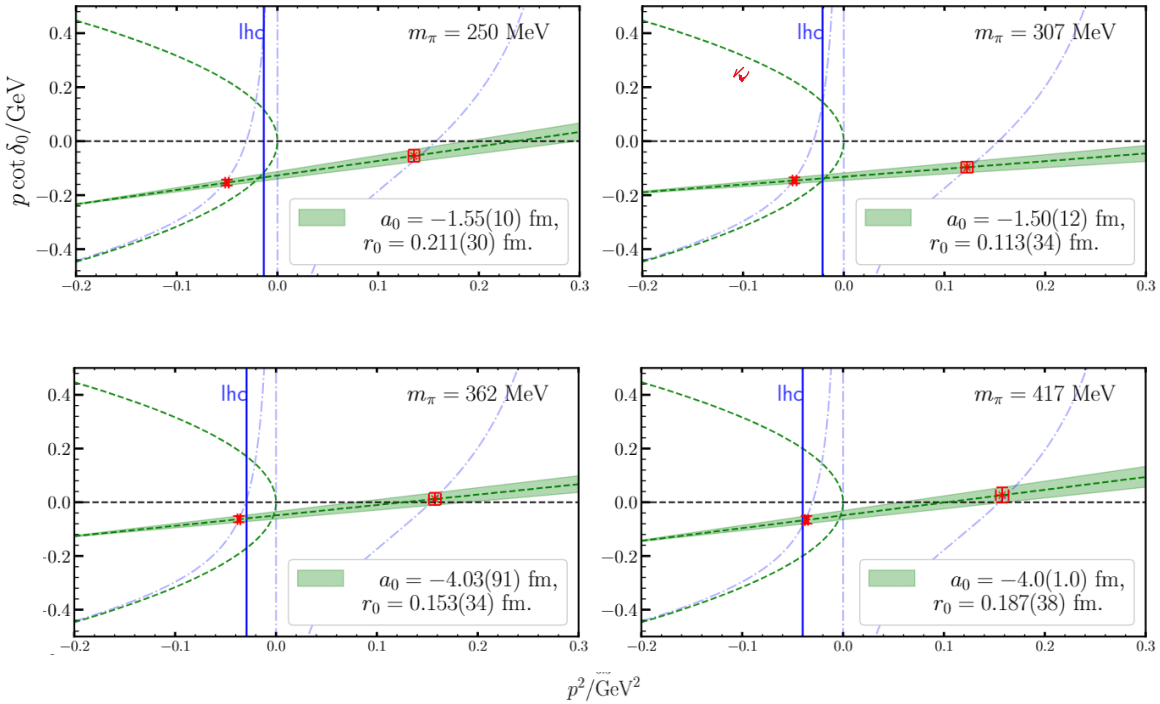
$$a_0^{DD^*} = -1.7 \pm 0.4\ \text{fm}\ , \quad r_0^{DD^*} = 0.5 \pm 0.1\ \text{fm}$$

$X(3872)$	$m_X - \frac{1}{4}(m_{\eta_c} + 3m_{J/\psi})$	$m_X - (m_{D^0} + m_{D^{0*}})$
$\text{lat}^{L\to\infty}$	815 ± 7 MeV	-11 ± 7 MeV
exp	804 ± 1 MeV	-0.14 ± 0.22 MeV

2. Lattice studies of $X(3872)$

H. Li et al. 2402.14541 [hep-lat]

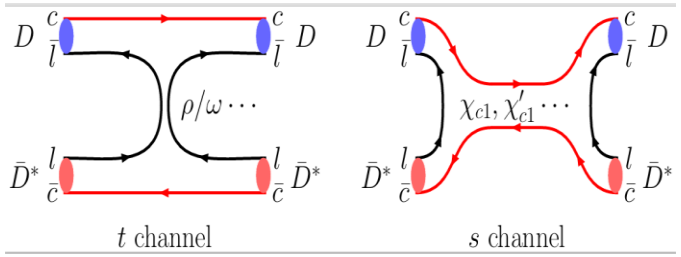


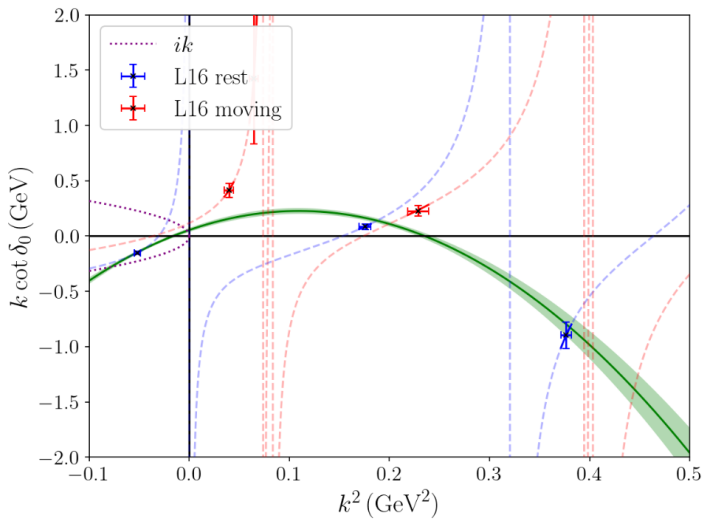


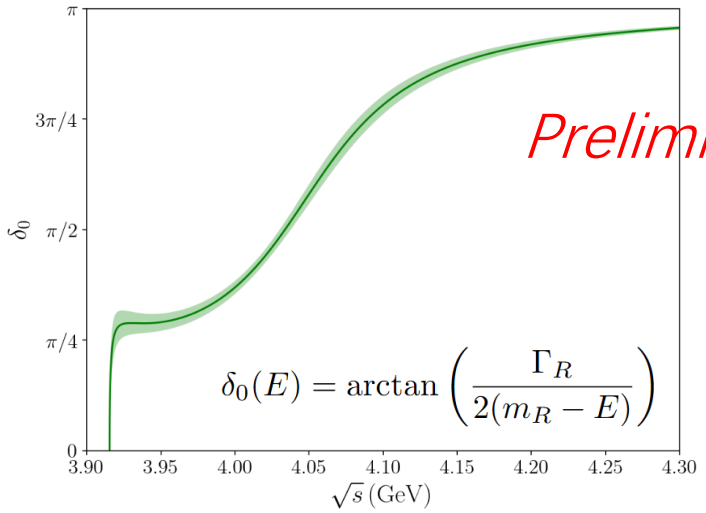
- S-wave $D\bar{D}^*(\mathrm{I}=0)$ scattering revisited at four m_π from 250 MeV to 420 MeV.
- Energy levels (totally three) are calculated in the rest frame
- A subthreshold bound state observed for all m_π when the left-hand-cut issue is ignored.
- However, each pole resides to the left of the left-hand-cut (indicated by the blue vertical lines)
- So the conclusion of a bound state is indefinite.

2. Lattice studies of $X(3872)$

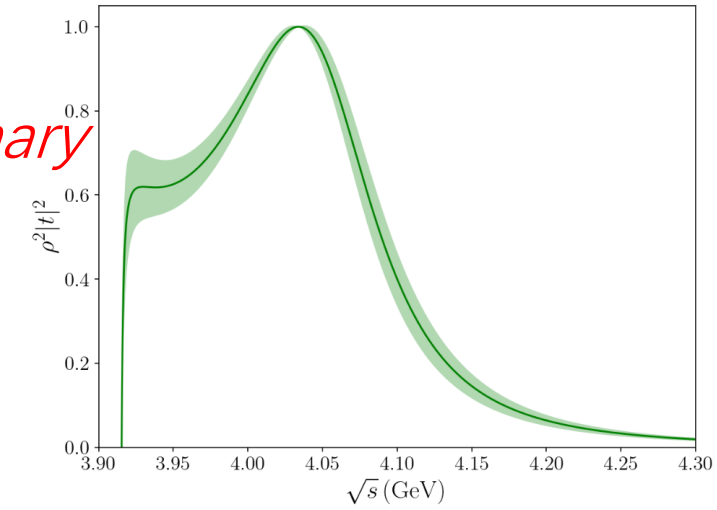
- The $D\bar{D}^*(\mathrm{I}=0)$ interaction :
- Moving frame FVEs are added to get the amplitude more constrained.
- A sub-threshold virtual state pole corresponding to X(3872)
- A resonance around 4.0 GeV likely corresponding the $\chi_{c1}{}'(4010)$
  (R. Aaij (LHCb Collab.), Phys. Rev. Lett. 133, 131902 (2024))







Preliminary



$$k\cot\delta_0(k) = \frac{1}{a_0} + \frac{1}{2}r_0k^2 + Ck^4$$

$a_0 \approx 3.63$ fm, $r_0 \approx 1.24$ fm

$C \approx -(0.48\,fm)^3$

Virtual pole:

$k \approx -0.047\,i$ GeV

$E_B = E - (m_{D^*} + m_D)$

≈ 1 MeV

Resonance pole:

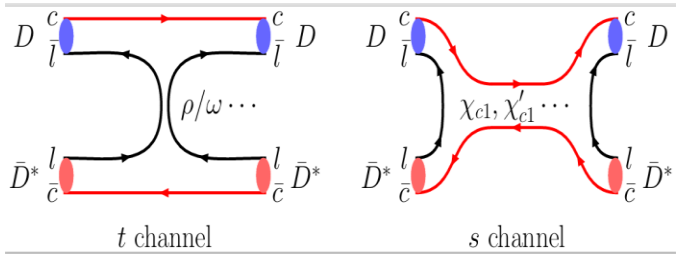
$k \approx (-0.522 \pm i0.116)$ GeV

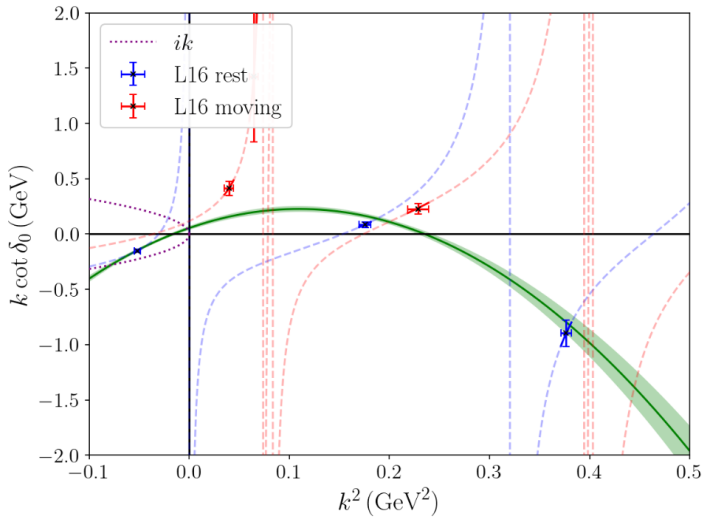
$\sqrt{s} = (4.046 - i\,0.060)$ GeV

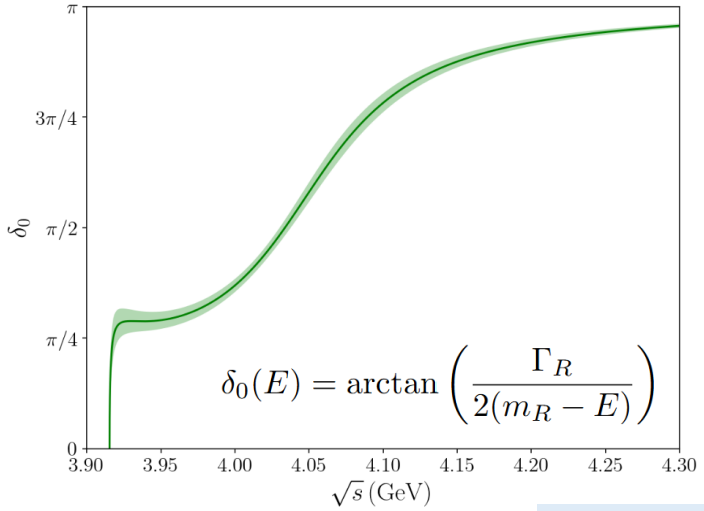
$(m_R, \Gamma_R) \approx (4.046, 0.12)$GeV

2. Lattice studies of $X(3872)$

- The $D\bar{D}^*(\mathrm{I}=0)$ interaction :
- Moving frame FVEs are added to get the amplitude more constrained.
- A sub-threshold virtual state pole corresponding to X(3872)
- A resonance around 4.0 GeV likely corresponding the $\chi_{c1}{}'(4010)$
  (R. Aaij (LHCb Collab.), Phys. Rev. Lett. 133, 131902 (2024))







- **Generalized Levinson' theorem:**
  $\delta_l(0^+) - \delta_l(p_{max}) = (n_l - n_b)\pi,$
  n_l: the number of bound states,
  n_b: the number of bare states below p_{max}.
  (F. Vidal et al., PRC45(1992)418,
  Y. Li et al.,PRD105(2022)116024)

$$k\cot\delta_0(k) = \frac{1}{a_0} + \frac{1}{2}r_0k^2 + Ck^4$$

$a_0 \approx 3.63$ fm, $r_0 \approx 1.24$ fm

$C \approx -(0.48\,fm)^3$

Virtual pole:

$k \approx -0.047\,i$ GeV

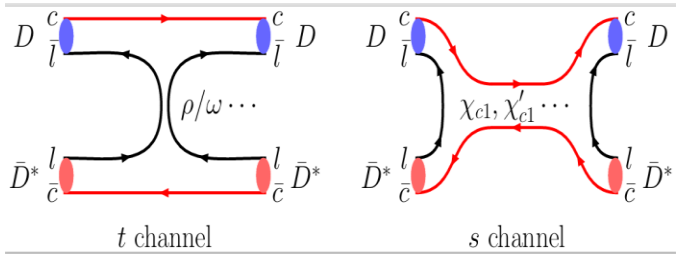
$E_B = E - (m_{D^*} +$

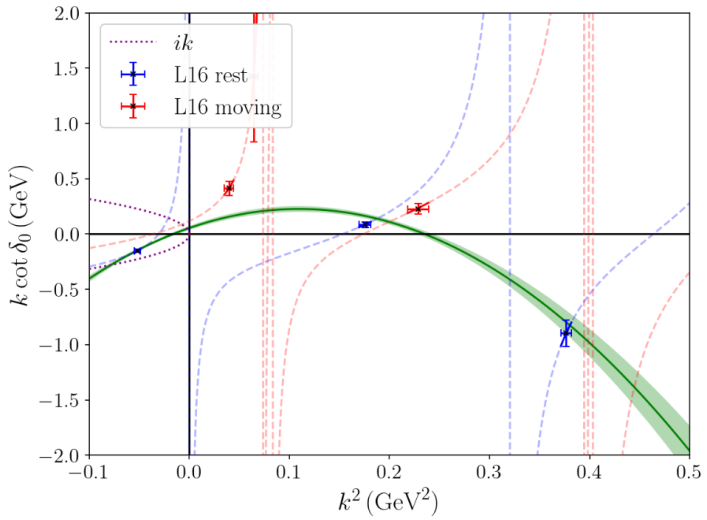
≈ 1 MeV

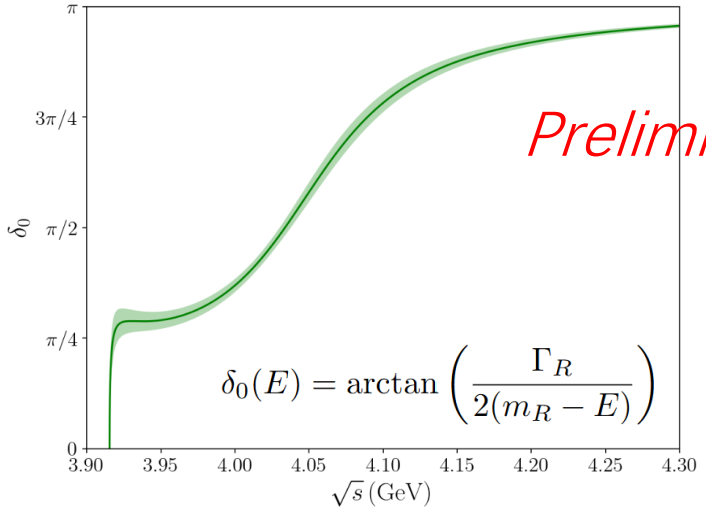
- ✓ Starts with $\delta_0(0^+) = 0$;
- ✓ Goes up rapidly due to the sub-th virtual state;
- ✓ Goes up when approaching $m_{\chi_{c1}(2P)}$;
- ✓ Goes up to $\delta_0(p) \approx \pi$ when passing $m_{\chi_{c1}(2P)}$.

2. Lattice studies of $X(3872)$

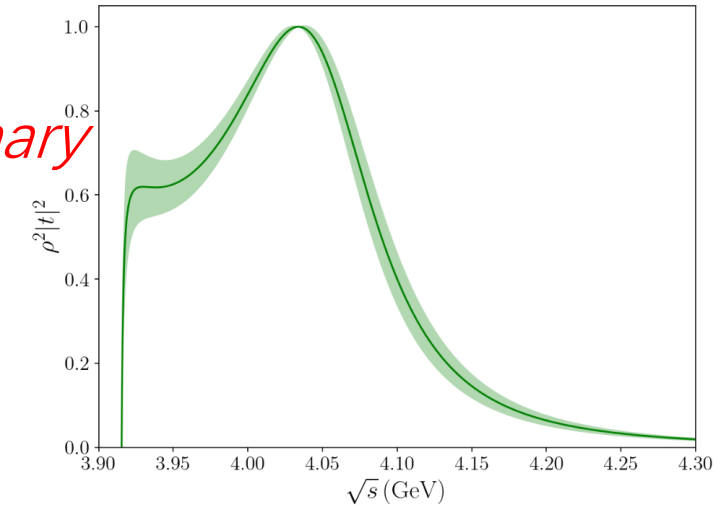
- The $D\bar{D}^*(\mathrm{I}=0)$ interaction :
- Moving frame FVEs are added to get the amplitude more constrained.
- A sub-threshold virtual state pole corresponding to X(3872)
- A resonance around 4.0 GeV likely corresponding the $\chi_{c1}{}'(4010)$
  (R. Aaij (LHCb Collab.), Phys. Rev. Lett. 133, 131902 (2024))







Preliminary



$$k\cot\delta_0(k) = \frac{1}{a_0} + \frac{1}{2}r_0k^2 + Ck^4$$

$a_0 \approx 3.63$ fm, $r_0 \approx 1.24$ fm

$C \approx -(0.48\,fm)^3$

Virtual pole:

$k \approx -0.047\,i$ GeV

$E_B = E - (m_{D^*} + m_D)$

≈ 1 MeV

Resonance pole:

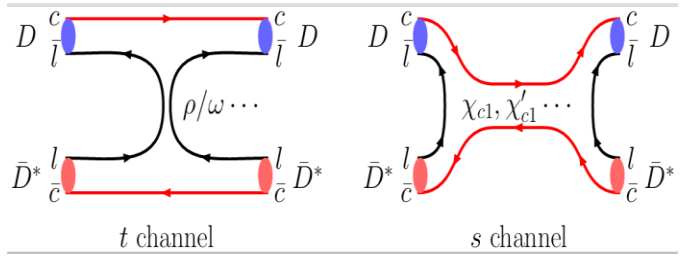
$k \approx (-0.522 \pm i0.116)$ GeV

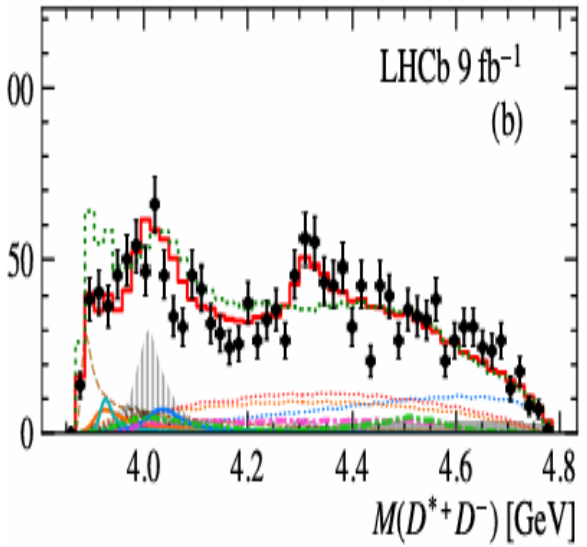
$\sqrt{s} = (4.046 - i\,0.060)$ GeV

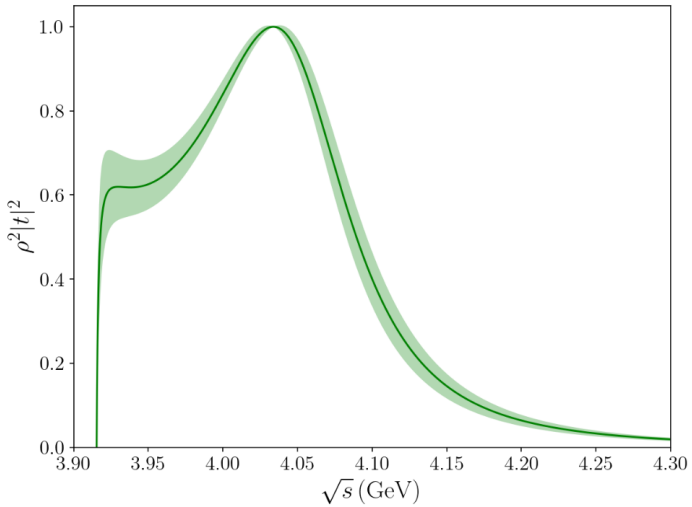
$(m_R, \Gamma_R) \approx (4.046, 0.12)$GeV

2. Lattice studies of $X(3872)$

- The $D\bar{D}^*(\mathrm{I}=0)$ interaction :
- Moving frame FVEs are added to get the amplitude more constrained.
- A sub-threshold virtual state pole corresponding to X(3872)
- A resonance around 4.0 GeV likely corresponding the $\chi_{c1}{}'(4010)$
  (R. Aaij (LHCb Collab.), Phys. Rev. Lett. 133, 131902 (2024))





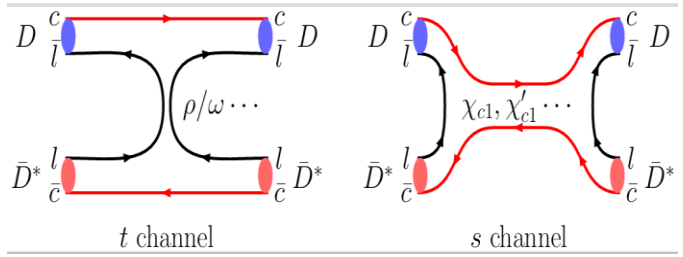


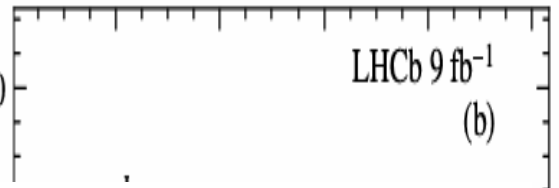
Resonance pole:

$$\boldsymbol{k \approx (-0.522 \pm i0.116)\ \mathrm{GeV}}$$
$$\boldsymbol{\sqrt{s} = (4.046 - i\,0.060)\ \mathrm{GeV}}$$
$$\boldsymbol{(m_R, \Gamma_R) \approx (4.046, 0.12)\mathrm{GeV}}$$

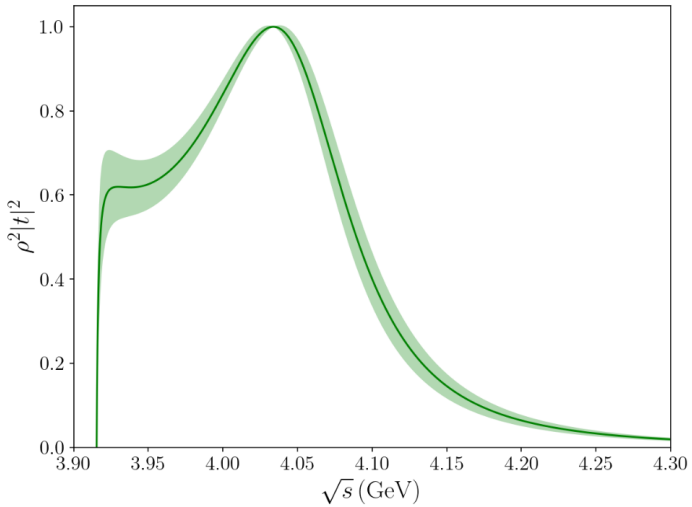
2. Lattice studies of $X(3872)$

- The $D\bar{D}^*(\mathrm{I}=0)$ interaction :
- Moving frame FVEs are added to get the amplitude more constrained.
- A sub-threshold virtual state pole corresponding to X(3872)
- A resonance around 4.0 GeV likely corresponding the $\chi_{c1}{}'(4010)$
  (R. Aaij (LHCb Collab.), Phys. Rev. Lett. 133, 131902 (2024))





This work		Known states [6]		$c\bar{c}$ prediction [34]	
$\eta_c(3945)$	$J^{PC}=0^{-+}$	$X(3940)$ [9,10]	$J^{PC}=?^{??}$	$\eta_c(3S)$	$J^{PC}=0^{-+}$
$m_0=3945\,^{+28\,+37}_{-17\,-28}$	$\Gamma_0=130\,^{+92\,+101}_{-49\,-70}$	$m_0=3942\pm9$	$\Gamma_0=37\,^{+27}_{-17}$	$m_0=4064$	$\Gamma_0=80$
$h_c(4000)$	$J^{PC}=1^{+-}$	$T_{c\bar{c}}(4020)^0$ [35]	$J^{PC}=?^{?-}$	$h_c(2P)$	$J^{PC}=1^{+-}$
$m_0=4000\,^{+17\,+29}_{-14\,-22}$	$\Gamma_0=184\,^{+71\,+97}_{-45\,-61}$	$m_0=4025.5\,^{+2.0}_{-4.7}\pm3.1$	$\Gamma_0=23.0\pm6.0\pm1.0$	$m_0=3956$	$\Gamma_0=87$
$\chi_{c1}(4010)$	$J^{PC}=1^{++}$			$\chi_{c1}(2P)$	$J^{PC}=1^{++}$
$m_0=4012.5\,^{+3.6\,+4.1}_{-3.9\,-3.7}$	$\Gamma_0=62.7\,^{+7.0\,+6.4}_{-6.4\,-6.6}$			$m_0=3953$	$\Gamma_0=165$
$h_c(4300)$	$J^{PC}=1^{+-}$			$h_c(3P)$	$J^{PC}=1^{+-}$
$m_0=4307.3\,^{+6.4\,+3.3}_{-6.6\,-4.1}$	$\Gamma_0=58\,^{+28\,+28}_{-16\,-25}$			$m_0=4318$	$\Gamma_0=75$
		$\chi_c(4274)$ [36]	$J^{PC}=1^{++}$	$\chi_{c1}(3P)$	$J^{PC}=1^{++}$
		$m_0=4294\pm4\,^{+6}_{-3}$	$\Gamma_0=53\pm5\pm5$	$m_0=4317$	$\Gamma_0=39$



Resonance pole:

$$k \approx (-0.522 \pm i0.116)\ \mathrm{GeV}$$
$$\sqrt{s} = (4.046 - i\,0.060)\ \mathrm{GeV}$$
$$(m_R, \Gamma_R) \approx (4.046, 0.12)\mathrm{GeV}$$

III. T_{bb} counterpart of $T_{cc}^{+}(3875)$

A. BB potential and $\bar{b}\bar{b}ud$ $\left(I(J^P) = 0(0^+)\right)$ tetraquark bound states using lattice QCD

- Static anti-heavy quarks
- The $r_{\bar{b}\bar{b}}$ dependence of the BB system defines the potential.
- The Schrödinger equation is solved to give the binding energy.
- A bound state exists in the $I(J^P) = 0((0,1)^+)$ channel

$$E_B = -90^{+43}_{-36}\ \text{MeV}$$

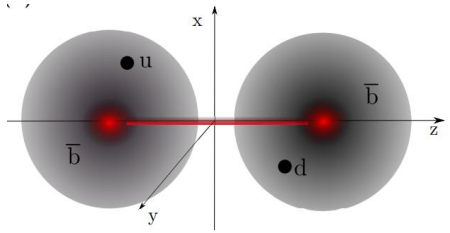
and no binding in the $I(J^P) = 1(1^+)$ channel.

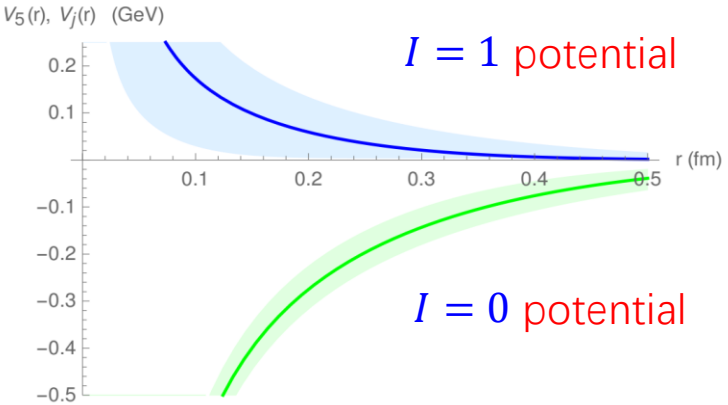
(P. Bicudo et al. Phys. Rev. D 93 (2016) 034507)

- A bound state exists in the $I(J^P) = 0(1^+)$ DD^* and D^*D^* coupled channel

$$E_B = -59^{+30}_{-38}\ \text{MeV}$$

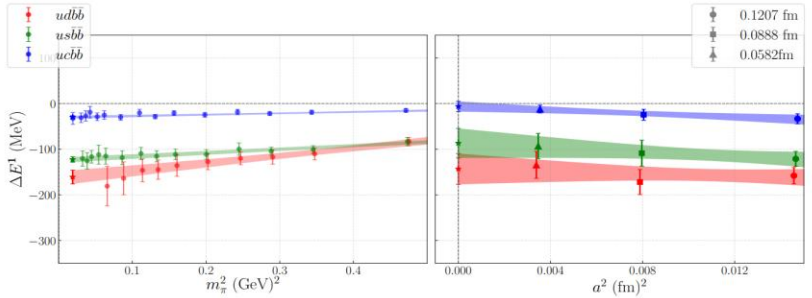
(P. Bicudo et al. Phys. Rev. D 95 (2017) 034502)





B. $\bar{b}\bar{b}ud$ $\left(I(J^P) = 0(1^+)\right)$ tetraquark bound state hinted by negative binding energy

- Chiral extrapolation
- Continuum extrapolation

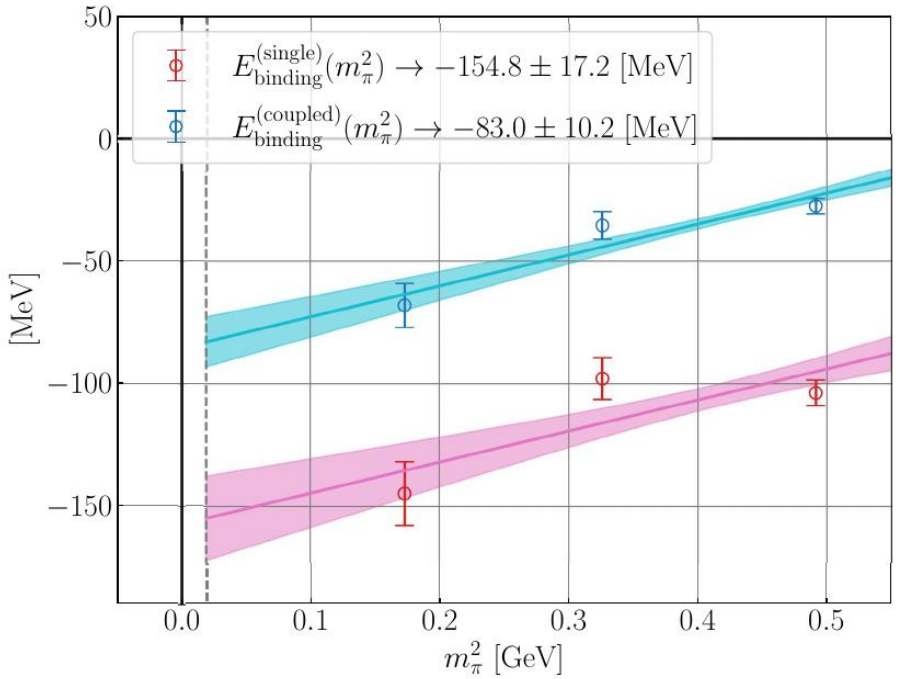


P. Junnarkar et al.,
Phys. Rev. D 99, 034507 (2019)

C. $\bar{b}\bar{b}ud$ $\left(I(J^P) = 0(1^+)\right)$ tetraquark bound state from $BB^* - B^*B^*$ coupled channel analysis

Aoki, Aoki & Inoue, Phys. Rev. D 108, 054502 (2023)

- BB* and B*B* potentials are extracted using HALQCD formalism at three pion masses of about 410–700 MeV (NRQCD bottom quarks). T
- An $I(J^P) = 0(1^+)$ bound state is confirmed.
- Extrapolation to physical m_π gives a binding magnitude of 83 ± 10 MeV in the coupled analysis, compared with 155 ± 17 MeV in a single-channel treatment.
- The difference shows the importance of channel coupling..

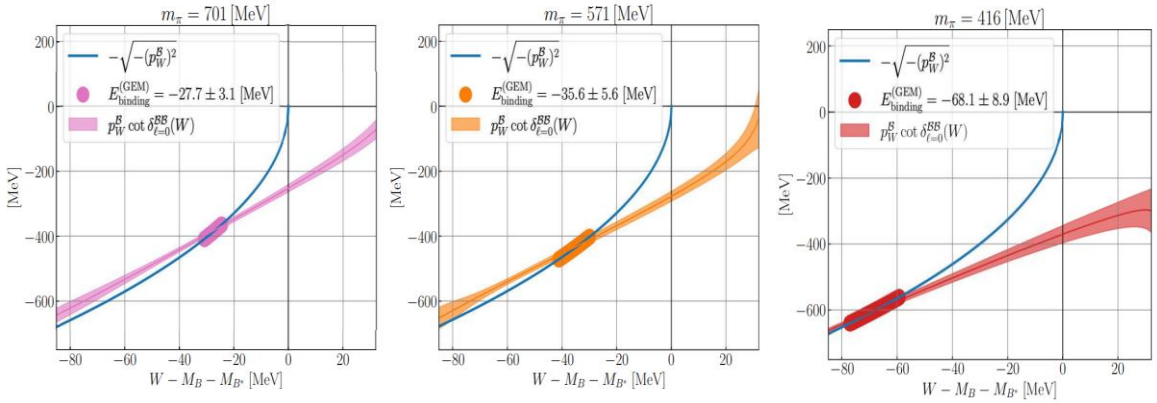


Physical-pion extrapolation with one channel and with coupled channels

The plotted errors do not include every systematic effect. The paper estimates additional uncertainty of order 20 MeV.

[13] arXiv:2306.03565 · Original figure 5

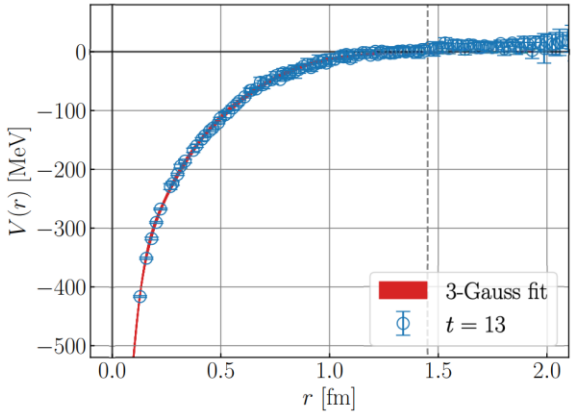
- Calculate the NBS wave function to derive the potential of $BB^* - B^*B^*$ coupled channel potential.
- Solve the Lippmann-Schwinger equation to get the scattering phase of the BB^* single channel.

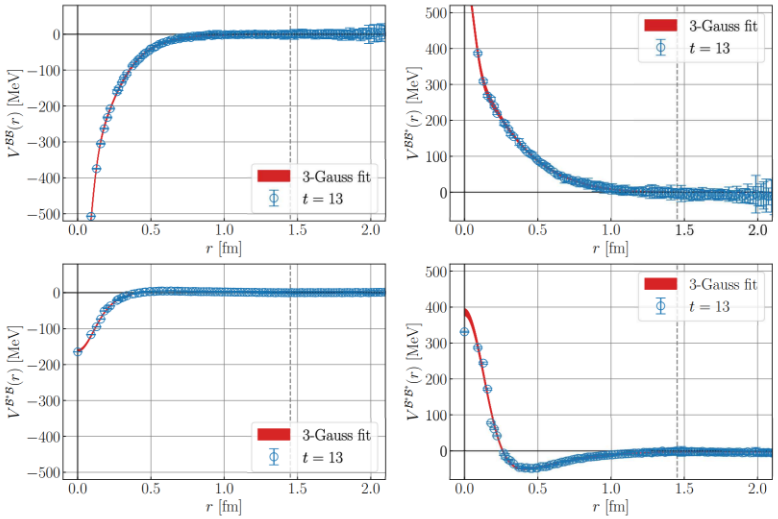


- The linear chiral extrapolation of the binding energy in m_π^2 gives

$$E_B^{\text{single}} = -154.8 \pm 17.2\ \text{MeV},$$
$$E_B^{\text{couple}} = -83.0 \pm 10.2\ \text{MeV}$$

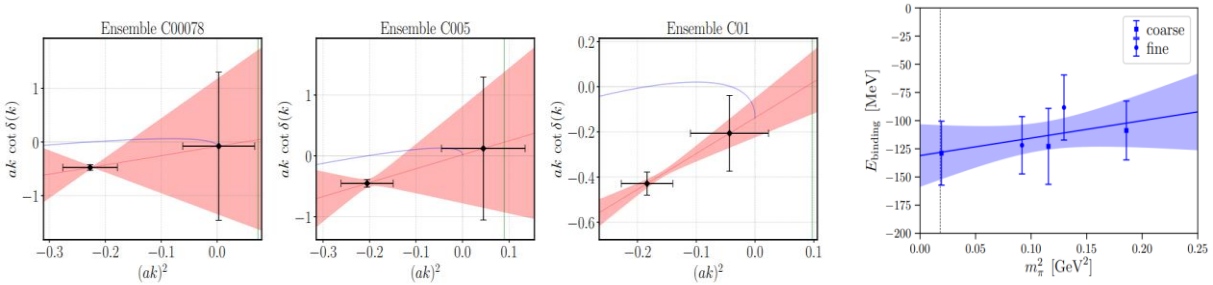
- Corroborate the previous lattice results.





D. $\bar{b}\bar{b}ud\ \left(I(J^P) = 0(1^+)\right)$ tetraquark bound state with meson-meson and local tetraquark operators

- For the $\bar{b}\bar{b}ud\ (0(1^+))$ system, phase shifts $\delta_0(k)$ are calculated at five m_π values.



All the cases give negative E_B, which are extrapolated to the value at the physical m_π:

$$E_B = -128 \pm 24 \pm 10\ \text{MeV}$$

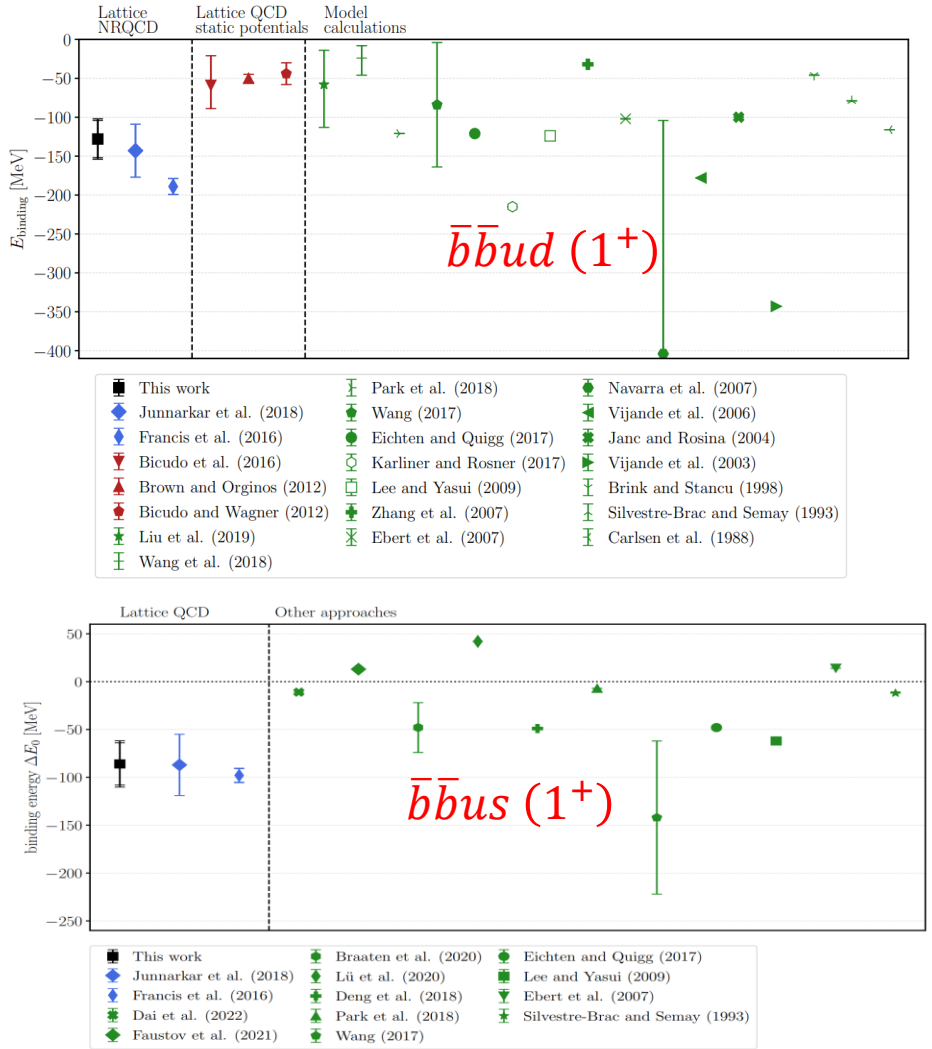
(L. Leskovec et al. Phys. Rev. D 100 (2019) 014503)

- Clear evidence for a $\bar{b}\bar{b}us\ (1^+)$ tetraquark:

$$E_B = -86 \pm 22 \pm 10\ \text{MeV}$$

but strong discrepancies, even on the qualitive level, between non-lattice results.

(S. Meinel et al. Phys. Rev. D 106 (2022) 034507)

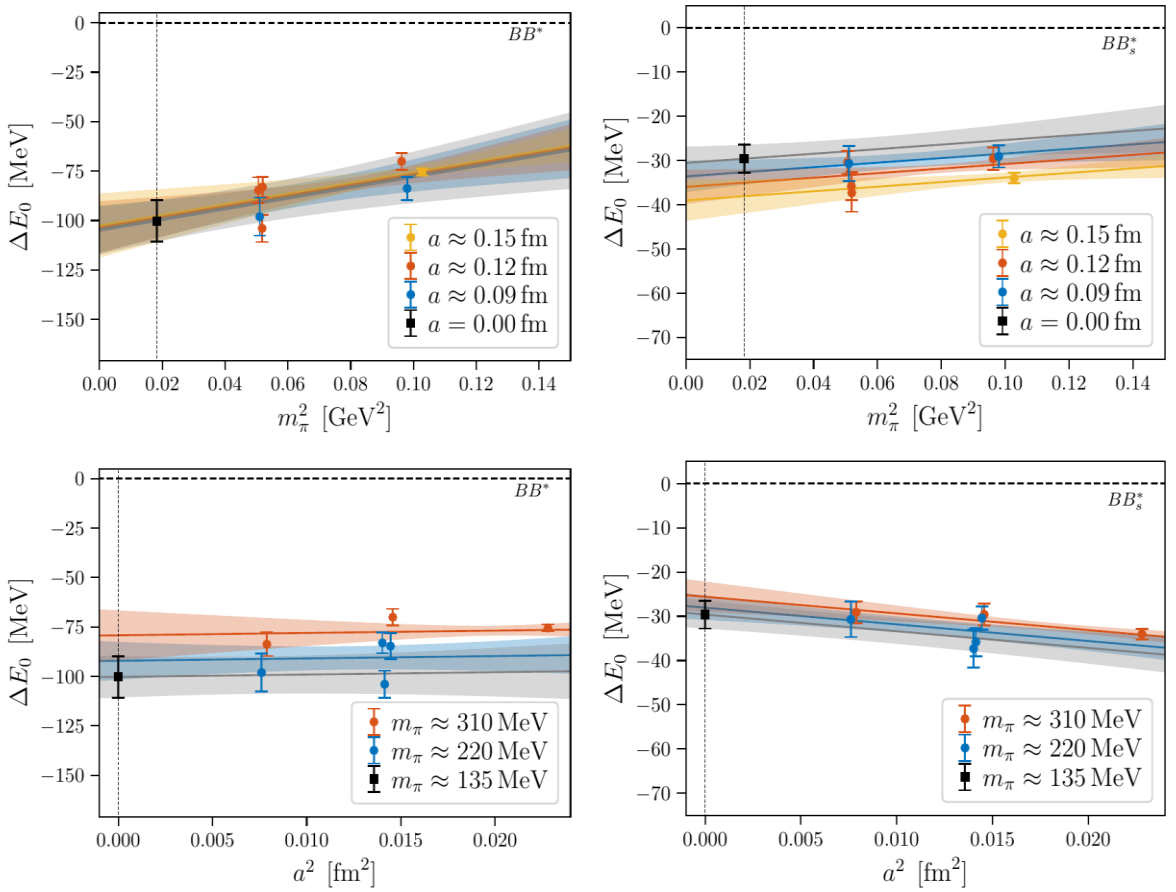


Blue: LQCD, Green: Pheno.

E. $\bar{b}\bar{b}ud\ \left(I(J^P) = 0(1^+)\right)$ tetraquark bound state with meson-meson and local tetraquark operators

Alexandrou et al., Phys. Rev. D 110, 054510 (2024)

- Both local $\mathcal{O}^{4q}$ and $B^*B^{(*)}$ operators are involved .
- $\bar{b}\bar{b}ud\ \left(I(J^P) = 0(1^+)\right)$ bound state and $\bar{b}\bar{b}us\ \left(I(J^P) = \frac{1}{2}(1^+)\right)$ bound state are observed.
- Combined chiral and lattice-spacing extrapolations give central energy shifts of about −100 and −30 MeV, respectively.



Chiral and continuum extrapolations for the light–light and light–strange channels

F. Electromagnetic Form Factors and Structure of the T_{bb} Tetraquark from Lattice QCD

S. Prelovsek, Phys. Rev. Lett. 136, 161901 (2026)

- **Tetraquark operator**: $[bb]_1^{3^*,S}[\bar{u}\bar{d}]_0^{3,A}$

$$\mathcal{O}^\dagger_{T_{bb}}(x,i) = \epsilon^{abc}\epsilon^{ade}[\bar{b}(x)_b C\gamma_i \bar{b}(x)_c][u(x)_d C\gamma_5 d(x)_e]$$

- **The matrix elements of j^μ_{EM} between T_{bb}**:

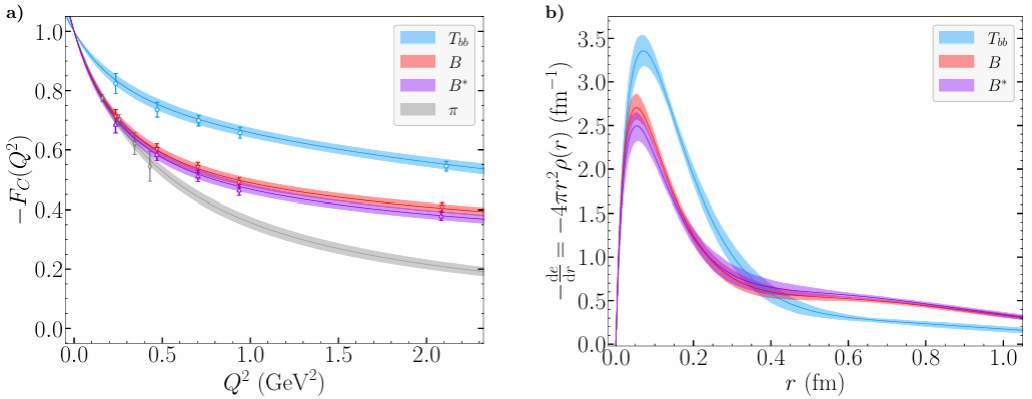
$$m_{T_{bb}} - (m_B + m_{B^*}) = -64(10)\ \text{MeV}$$

$$\mathcal{M}^\mu_{EM}(p_2,\lambda_2,p_1,\lambda_1) = \langle h(p_2,\lambda_2)|\hat{j}^\mu_{EM,cont}|h(p_1,\lambda_1)\rangle,$$

$$\hat{j}^\mu_{EM,cont} = \sum e_q \bar{q}\gamma^\mu q, \qquad (1)$$

- **The form factors:**

$$\mathcal{M}^\mu_{EM} = -(p_1+p_2)^\mu(\varepsilon_2^*\cdot\varepsilon_1)F_1(Q^2) - \\ -[(\varepsilon_2^*\cdot q)\varepsilon_1^\mu - (\varepsilon_1\cdot q)\varepsilon_2^{*\mu}]F_2(Q^2) + \\ +\frac{(\varepsilon_2^*\cdot q)(\varepsilon_1\cdot q)}{2m^2}(p_1+p_2)^\mu F_3(Q^2),$$



$$\rho(r) = \int \frac{d^3\vec{q}}{(2\pi)^3}\, e^{i\vec{q}\cdot\vec{r}} F_C(|\vec{q}^2|)$$

$F_C(Q^2)$: charge FF
$F_M(Q^2)$: magnetic dipole FF
$F_Q(Q^2)$: electric quadruple FF

$$\begin{pmatrix} F_C(Q^2) \\ F_M(Q^2) \\ F_Q(Q^2) \end{pmatrix} = \begin{pmatrix} 1+\frac{2}{3}\eta & -\frac{2}{3}\eta & \frac{2}{3}\eta(1+\eta) \\ 0 & 1 & 0 \\ 1 & -1 & (1+\eta) \end{pmatrix} \begin{pmatrix} F_1(Q^2) \\ F_2(Q^2) \\ F_3(Q^2) \end{pmatrix} \qquad \eta = \frac{Q^2}{4M^2}$$

Authors interpretation:

- A bound state made up of a compact $[bb]^{3^*}_{S=1}$ diquark and a much larger $[\bar{u}\bar{d}]^{3}_{S=0}$ scalar diquark
- The charge radius of T_{bb} is substantially smaller than that of B and B^*

$$\sqrt{\langle r_C^2 \rangle} = \sqrt{6 \cdot \frac{\mathrm{d}F_C}{\mathrm{d}Q^2}(0)}$$

h	m_h (GeV)	$\sqrt{\langle r_C^2 \rangle}$ (fm)	r	t_+
T_{bb}	10.5765(98)	0.499(31)	ω	$(3m_\pi)^2$
B	5.3020(17)	0.692(21)	ρ	$(2m_\pi)^2$
B^*	5.3387(20)	0.698(23)	ρ	$(2m_\pi)^2$
π	0.28953(97)	0.652(20)	ρ	$(2m_\pi)^2$

	T_{bb}	$[bb]$	$[\bar{u}\bar{d}]$
$\sqrt{\langle r_C^2 \rangle}$ (fm)	0.499(31)	0.174(59)	0.511(14)
$2m_{T_{bb}} \cdot \mu$	1.912(57)	1.887(29)	0.02(18)
$m^2_{T_{bb}} \cdot \mathcal{Q}$	1.9(8.7)	0.6(8.8)	−0.18(86)

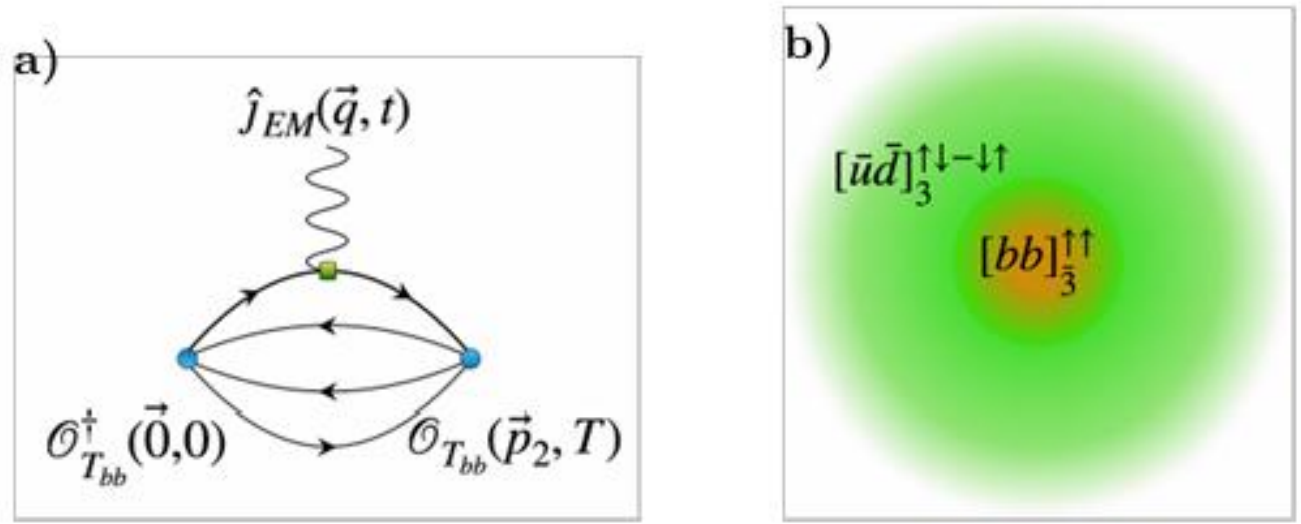
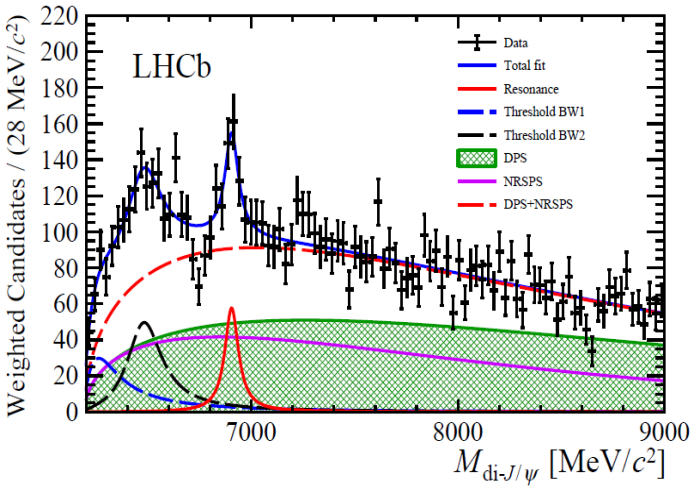
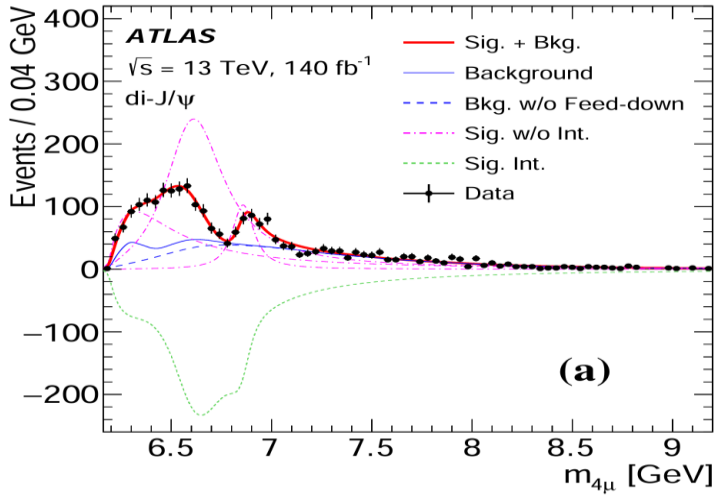


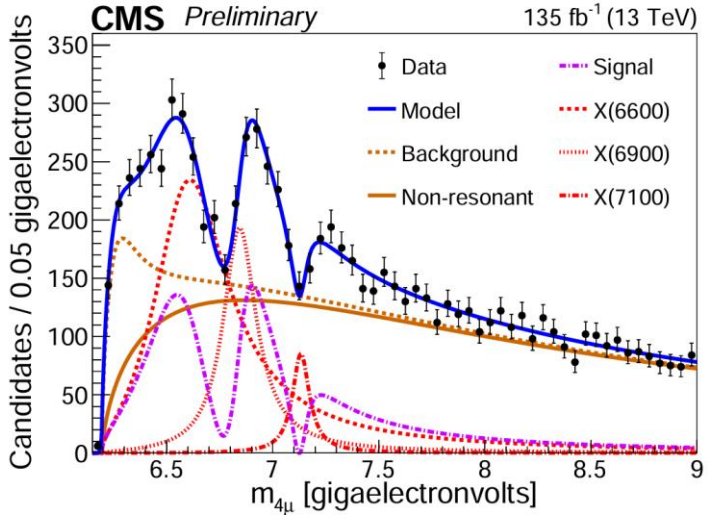
FIG. 1. **a)** Example of a connected Wick contraction diagram generated by the T_{bb} three-point correlator (6). **b)** Pictorial representation of the resulting distributions for light and heavy quarks.

IV. Fully charm tetraquarks and di-charmonium scatterings

1. Fully charmed tetraquark systems observed by LHCb, ATLAS and CMS







LHCb, Sci. Bull. 65 (2020) 1983 ATLAS, PRL. 131 (2023) 151902 CMS, PRL. 132 (2024) 111901

- **X(6900) first observed by LHCb in $J/\psi J/\psi$ spectrum in 2020, and confirmed by ATLAS (2023) and CMS (2024)**
- **ATLAS also observed X(6400) and (or) X(6600). CMS observed X(6600) and X(7100).**
- **Many phenomenological studies (fully charmed tetraquarks, di-charmonium resonances, etc.)**
- **CMS sorts X(6600), X(6900) and X(7100) into a tetraquark family with quantum numbers 2^{++}.**
- **Can be investigated in the formalism of lattice QCD**

		BW_1	BW_2	BW_3
Interference	m (MeV)	$6593\ ^{+15}_{-14} \pm 25$	$6847\ ^{+10}_{-10} \pm 15$	$7173\ ^{+9}_{-10} \pm 13$
(Run 2+Run 3)	Γ (MeV)	$446\ ^{+66}_{-54} \pm 87$	$135\ ^{+16}_{-14} \pm 14$	$73\ ^{+18}_{-15} \pm 10$
Interference	m (MeV)	$6638\ ^{+43+16}_{-38-31}$	$6847\ ^{+44+48}_{-28-20}$	$7134\ ^{+48+41}_{-25-15}$
(Run 2 [12])	Γ (MeV)	$440\ ^{+230+110}_{-200-240}$	$191\ ^{+66+25}_{-49-17}$	$97\ ^{+40+29}_{-29-26}$

We have extended our study of the J/ψJ/ψ mass spectrum with 3.6 times more J/ψJ/ψ pairs. The spectrum is well described by mutually interfering X(6600), X(6900), and X(7100) structures. The statistical uncertainties on their masses and widths are reduced by a factor of three over our previous results [12]. For the first time, all three structures are established with a significance well above five standard deviations (5σ). Similarly, interference among the three structures is now statistically compelling. Interference implies that the structures have common J^{PC} quantum numbers—suggesting a family of states. Recently CMS reported an angular analysis of the X$\rightarrow$J/ψJ/ψ decay characteristics and found the J^{PC} quantum numbers of the X family is most likely 2^{++} [35].

2. Lattice QCD calculations on relevant di-charmonium scatterings

G. Li et al., Phys. Rev. D 114, L031506 (2026); Phys.Rev.D 114, 034512 (2026)

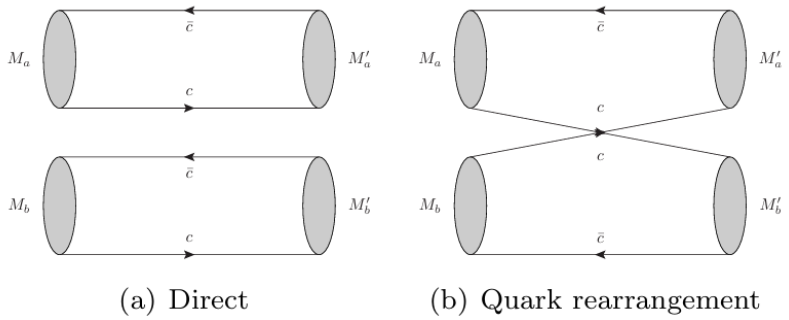
- Operator sets for 0^{++} and 2^{++} channels

$$\mathcal{S}_0 = \{\mathcal{O}_{\eta_c\eta_c}(n^2), \mathcal{O}_{\psi\psi}(n^2); n^2 = 0,1,2,3,4\},$$
$$\mathcal{S}_2 = \{\mathcal{O}_{\eta_c\eta_c}(n^2 \neq 0,3), \mathcal{O}_{\psi\psi}(n^2); n^2 = 0,1,2,3,4\}$$

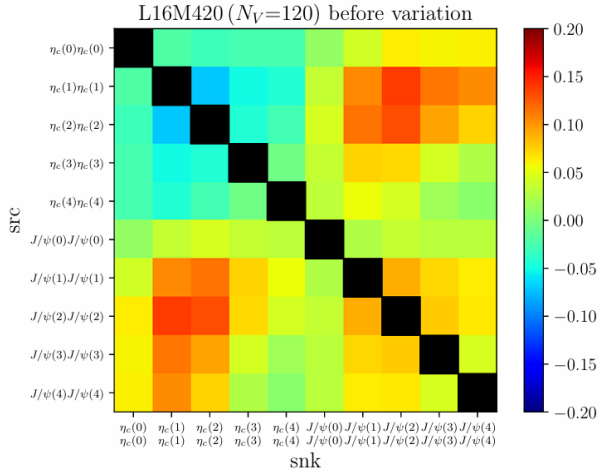
- Finite volume energy levels can be obtained by solving the generalized eigenvalue problem

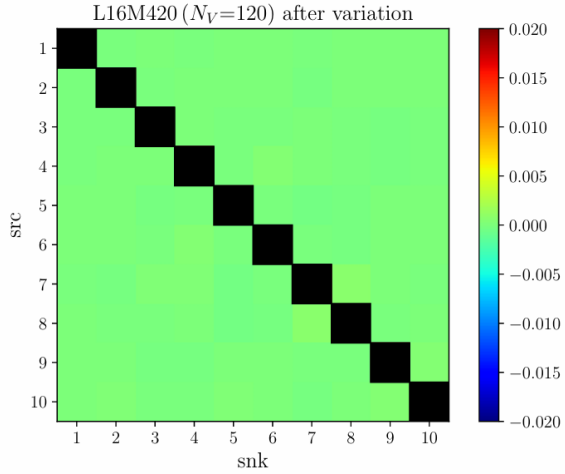
$$C_{\alpha\beta}(t) = \langle \mathcal{O}_\alpha(t)\mathcal{O}_\beta(0)\rangle$$

$$C_{\alpha\beta}(t_1)v_\beta^{(n)} = \lambda^{(n)}C_{\alpha\beta}(t_0)v_\beta^{(n)}$$



(a) Direct (b) Quark rearrangement





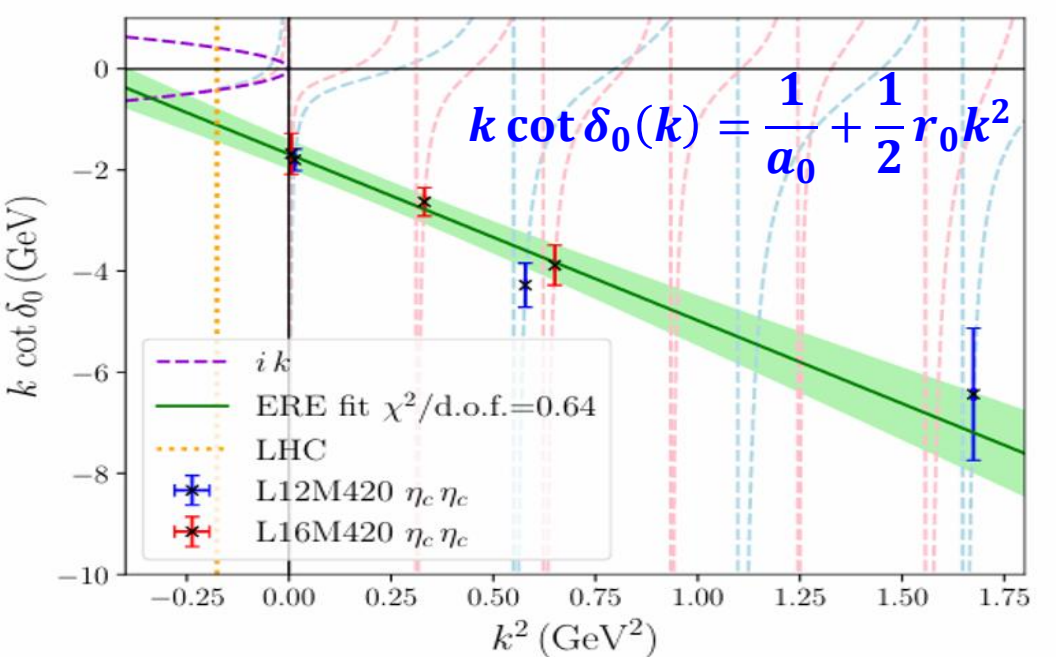
Optimized operator for the state $|n\rangle$

$$\mathcal{O}^{(n)} = v_\beta^{(n)}\mathcal{O}_\beta, \qquad \mathcal{O}^{(n)}|0\rangle = |n\rangle$$

$$C_{mn}(t) = \langle \mathcal{O}^{(m)}(t)\mathcal{O}^{(n)}\rangle \approx \delta_{mn}e^{-E_n t}$$

3. S-wave $\eta_c\eta_c$ and $J/\psi J/\psi$ scatterings in 0^{++} channel

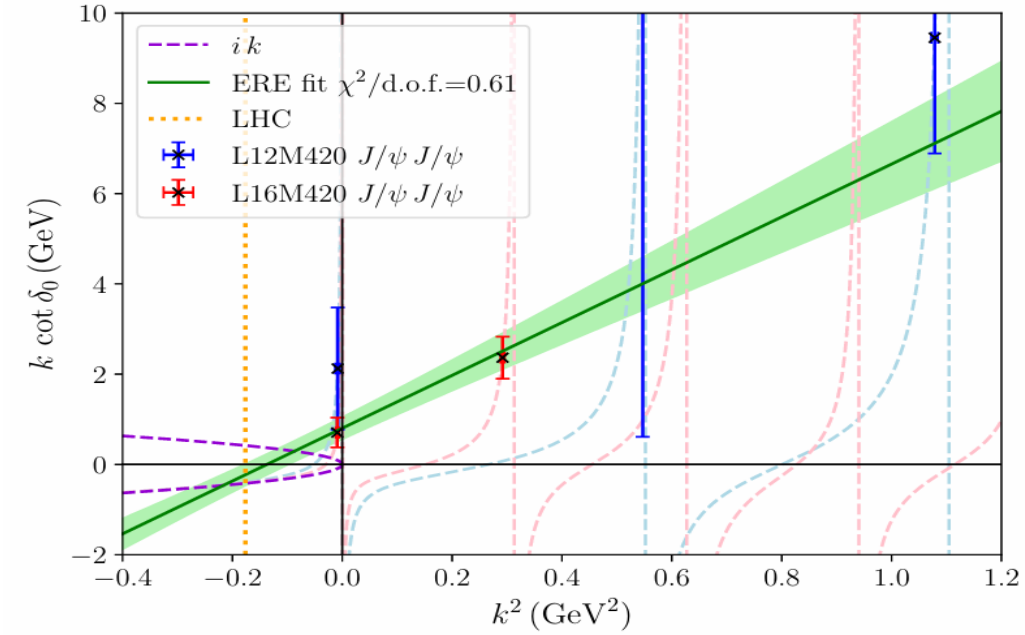
$\eta_c\eta_c$ scattering phase shift



- $a_0 = -0.117(19)$ fm , $r_0 = -1.30(20)$ fm
- Repulsive interaction (no sub-threshold energy level)
- The pole is to the left of the left hand cut (lhc)

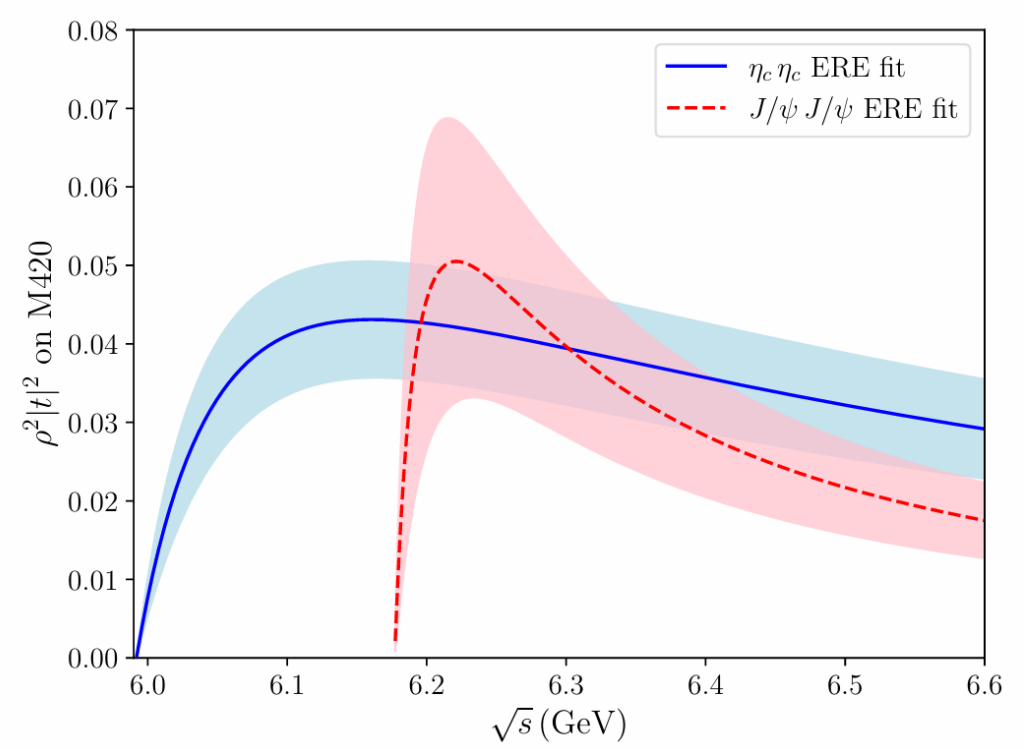
  $k_{lhc}^2 < \frac{m_\sigma^2}{4} \sim m_\pi^2$

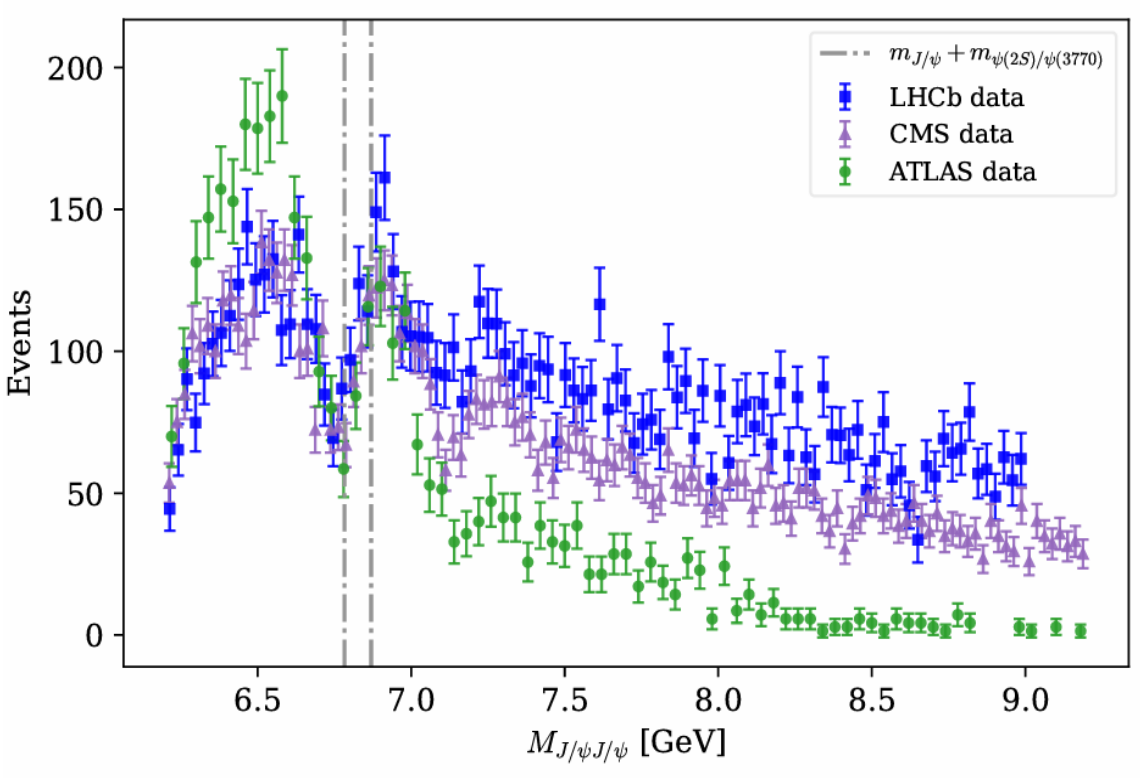
$J/\psi J/\psi$ scattering phase shift



- $a_0 = 0.25(7)$ fm , $r_0 = 2.31(33)$ fm
- Repulsive interaction , a virtual bound state pole
- Its existence is affected by the lhc position
- No definite conclusion can be drawn yet on the position of the pole.

A rapid rise at the threshold usually hints at the existence of a near threshold structure (not kinematic cusp)

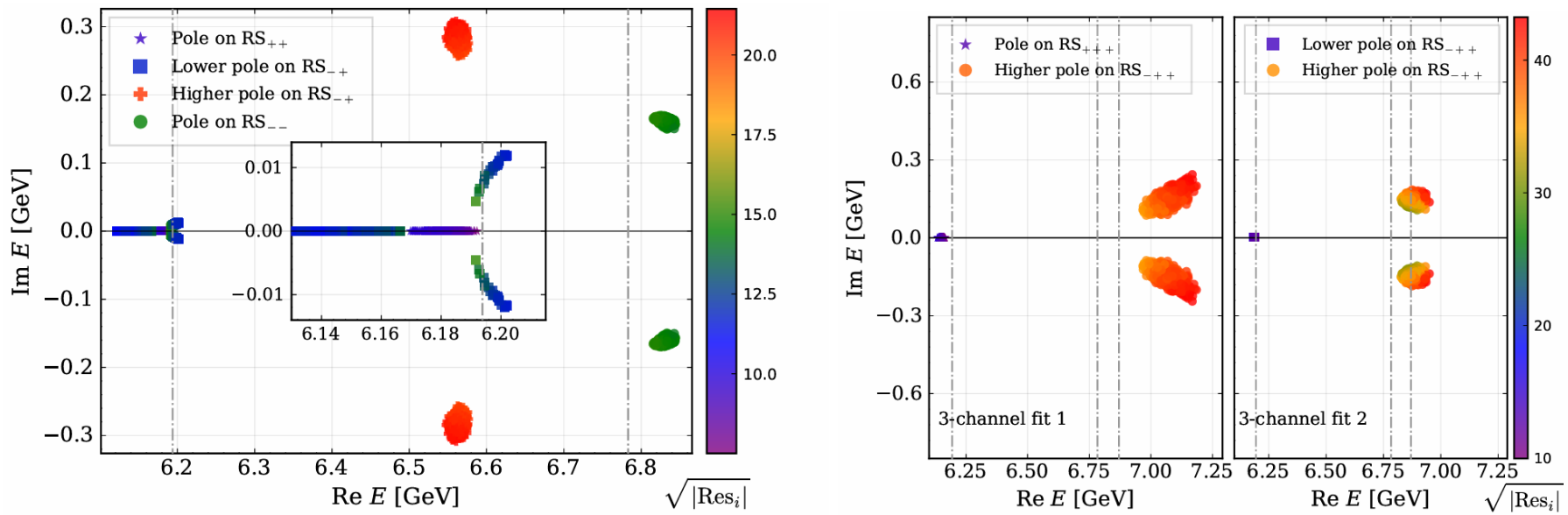




The attractive interaction is compatible with X(6200) predicted by a coupled-channel analysis to the experimental spectrum (X.-K. Dong, PRL 127 (2021) 119901; Y.-L. Song et al. *PRD* 111 (2025) 034038**)**

Table IV. Pole positions (in MeV) for the models employed in the analysis. The Riemann sheets (RSs) quoted in parentheses are tagged with the signs of the imaginary parts of the momenta in all channels relevant for the particular model.

Model	Two-channel fit	Three-channel fit 1	Three-channel fit 2
$X(6200)$	$[6171, 6194]$ (RS_{++}) or $[6124, 6202] - i[0, 12]$ (RS_{-+})	6151^{+12}_{-16} (RS_{+++})	6189^{+3}_{-6} (RS_{-++})
$X(6900)$	$6831^{+15}_{-17} - i162^{+8}_{-12}$ (RS_{--})	$7071^{+107}_{-101} - i147^{+81}_{-55}$ (RS_{-++})	$6872^{+77}_{-45} - i148^{+37}_{-43}$ (RS_{-++})
Other poles	$6564^{+13}_{-14} - i282^{+27}_{-27}$ (RS_{-+})	...	...



Our lattice result support X(6200) has the quantum numbers $J^{PC} = 0^{++}$

4. S-wave $J/\psi J/\psi$ scatterings in 2^{++} channel

- Singular behavior of $k\cot\delta_0(k)$.

- K-matrix parameterization

$$t^{-1}(s) = K^{-1}(s) - i\rho(s)$$

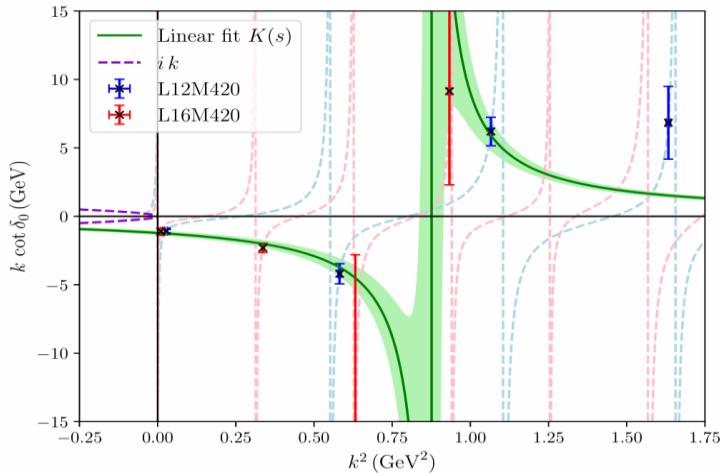
$$\sqrt{s}[k\cot\delta_0(k)]^{-1} = K(s)$$

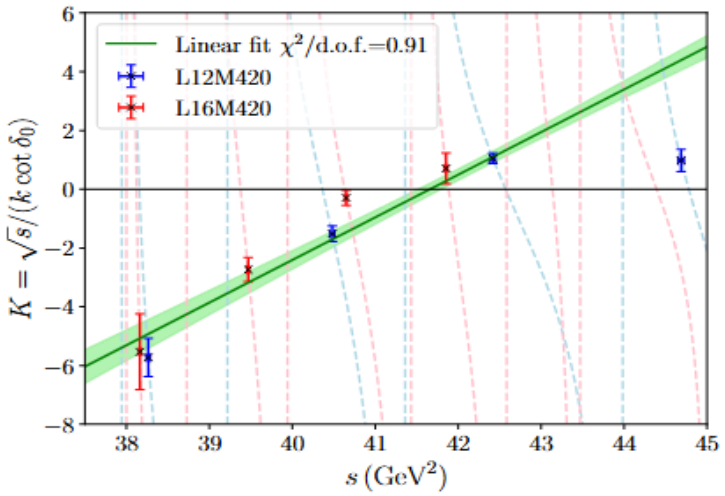
$$K(s) = a\,s + b$$

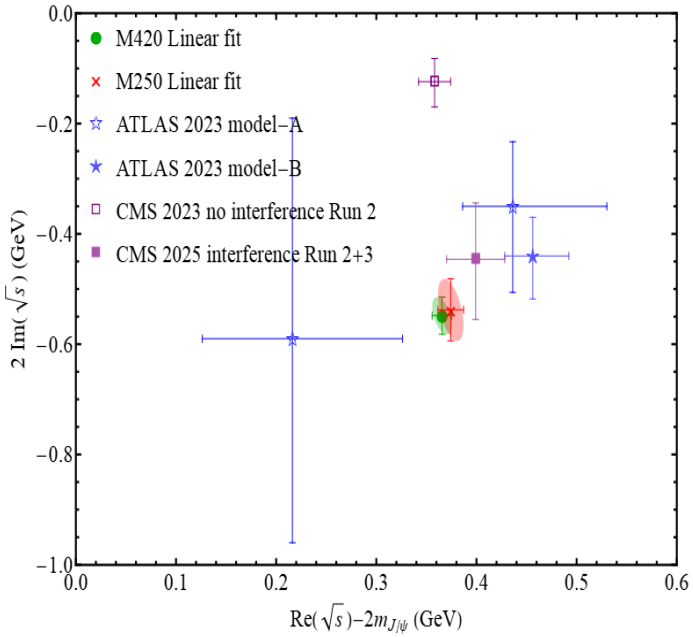
CDD zero: $s_0 = -b/a = (6.45(1)\ \text{GeV})^2$

- Pole singularity $t(s) = \dfrac{K(s)}{1 - iK(s)\rho(s)}$ $\quad t(s) \sim \dfrac{c_R^2}{s_R - s}$

$$\sqrt{s_R} = \left(6.543(10) - \frac{i}{2}\,0.548(34)\right)\ \text{GeV}$$



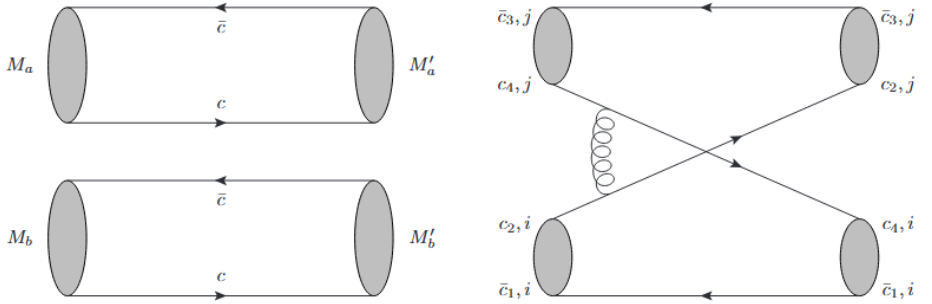




Our lattice result support X(6600) has the quantum numbers $J^{PC} = 2^{++}$

4. Di-charmonium interaction

- Quark diagrams contributing to the di-charmonium correlation functions



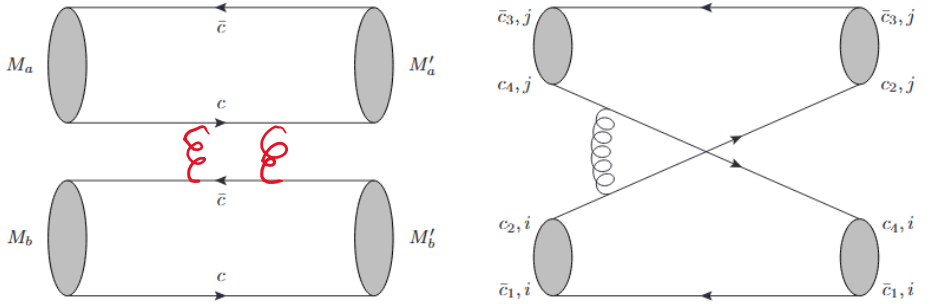
(a) Direct (D) (b) Quark rearrangement (Q)

4. Di-charmonium interaction

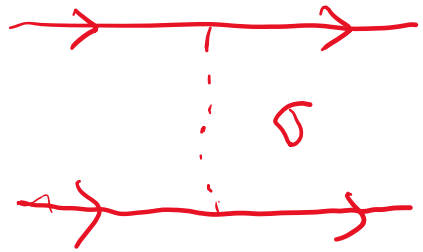
- Quark diagrams contributing to the di-charmonium correlation functions

$$C_{11}(t) = D(t) + Q(t) \equiv D^{(0)}(t) + D^{(1)}(t) + Q(t)$$

- The left diagram represents the gluon exchange or σ-exchange on the hadron level .



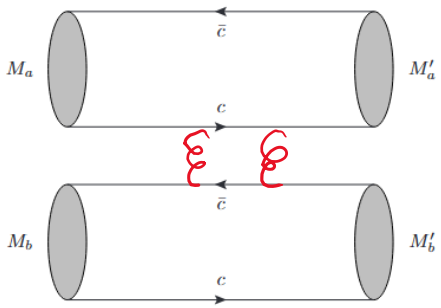
(a) Direct (D) (b) Quark rearrangement (Q)



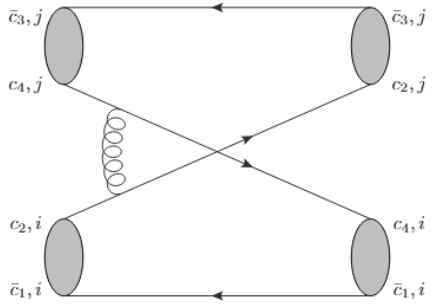
4. Di-charmonium interaction

- Quark diagrams contributing to the di-charmonium correlation functions

$$C_{11}(t) = D(t) + Q(t) \equiv D^{(0)}(t) + D^{(1)}(t) + Q(t)$$



(a) Direct (D)



(b) Quark rearrangement (Q)

- The left diagram represents the gluon exchange or σ-exchange on the hadron level .

- Comparing the contributions from the two diagrams

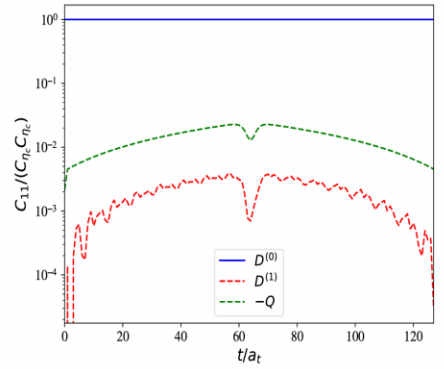
$$\frac{D^{(1)}(t)}{D^{(0)}(t)} \approx \epsilon_D e^{-\delta_D t}, \qquad \frac{Q(t)}{D^{(0)}(t)} \approx \epsilon_Q e^{-\delta_Q t}$$

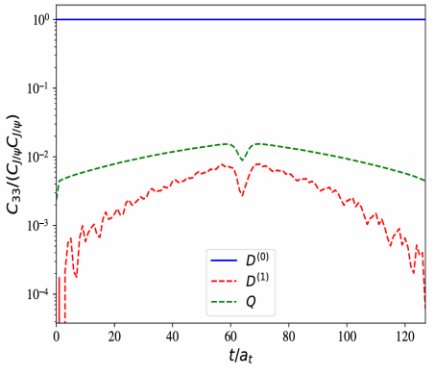
0^{++} $\eta_c\eta_c$

$$\delta_D < 0, \quad \epsilon_D \sim \mathcal{O}(10^{-3}),$$
$$\delta_Q < 0, \quad \epsilon_Q \sim -\mathcal{O}(10^{-2})$$

0^{++} $J/\psi J/\psi$

$$\delta_D < 0, \epsilon_D \sim \mathcal{O}(10^{-3})$$
$$\delta_Q < 0, \epsilon_Q \sim \mathcal{O}(10^{-2})$$





0^{++} $\eta_c\eta_c$: repulsive

0^{++} $J/\psi J/\psi$: attractive

- **Di-charmonium interaction is dominated by the charm quark rearrangement effect.**

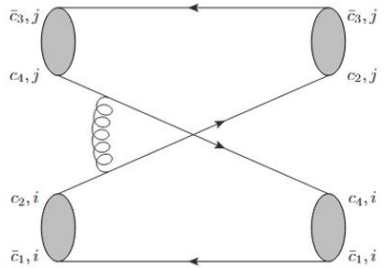
$$E_1 \approx \frac{1}{a_t} \ln \frac{C_{11}(t)}{C_{11}(t+a_t)}$$
$$\approx 2m_{\eta_c} + \epsilon_D \delta_D e^{\delta_D t} + \epsilon_Q \delta_Q e^{\delta_Q t}$$
$$\approx 2m_{\eta_c} + \epsilon_D \delta_D + \epsilon_Q \delta_Q,$$

0^{++} $\eta_c\eta_c$: repulsive $\quad E_1 - 2m_{\eta_c} \sim \epsilon_Q \delta_Q > 0$

0^{++} $J/\psi J/\psi$: attractive $\quad E_1 - 2m_{\psi} \sim \epsilon_Q \delta_Q < 0$

- **The different contributions of Q diagrams to 0^{++} $\eta_c\eta_c$ and 0^{++} $J/\psi J/\psi$**

Fierz rearrangement:



(b) Quark rearrangement (Q)

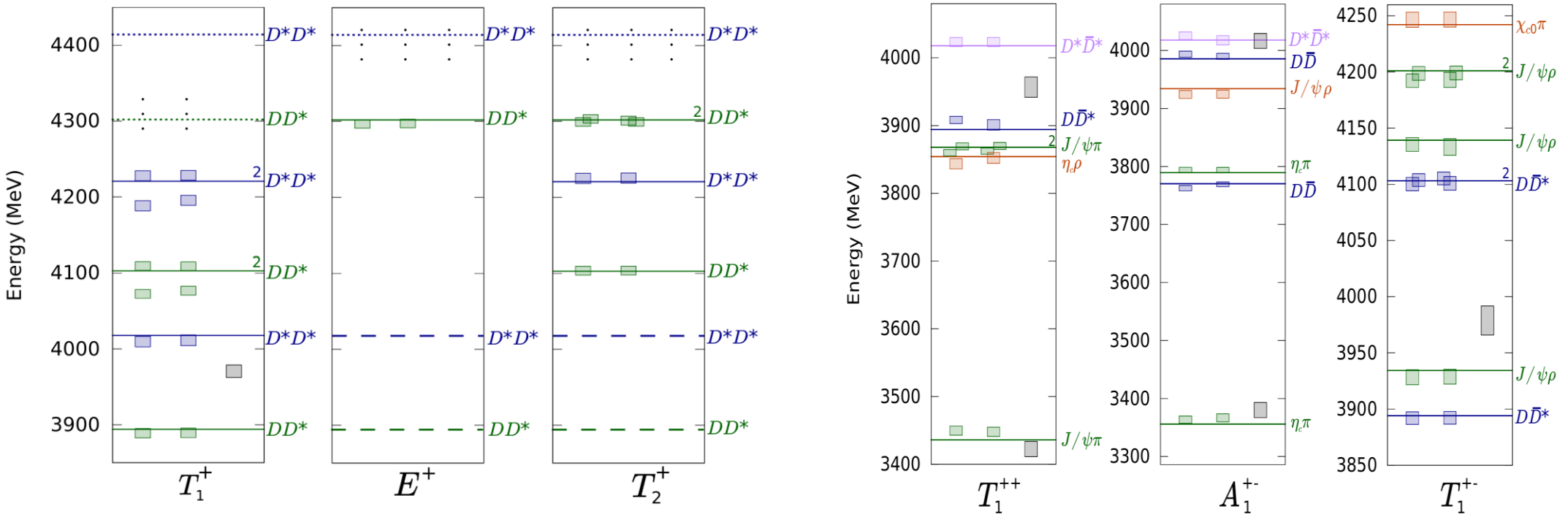
$$\bar{c}_1\gamma_5 c_2 \bar{c}_3\gamma_5 c_4 \to \frac{1}{4} \times \bar{c}_1\gamma_5 c_4 \bar{c}_3\gamma_5 c_2$$ 0^{++} $\eta_c\eta_c$

$$\bar{c}_1\gamma_\mu c_2 \bar{c}_3\gamma^\mu c_4 \to -\frac{1}{2} \times \bar{c}_1\gamma_\mu c_4 \bar{c}_3\gamma^\mu c_2$$ 0^{++} $J/\psi J/\psi$

V. Discussion on the relevance of local tetraquark operators

1. Doubly charmed and close-charmed tetraquark systems (T_{cc} and $X(3872)$)

- Experimentally, $T_{cc}^{+}(3875)$ and $X(3872)$ are very close in mass to the corresponding DD^{*} threshold.
- Theoretically, near-threshold pole singularities are derived for both cases.
- So the hadron-molecule interpretation seems more natural.
- As for the relevant of tetraquark operators——the completeness of operator sets.

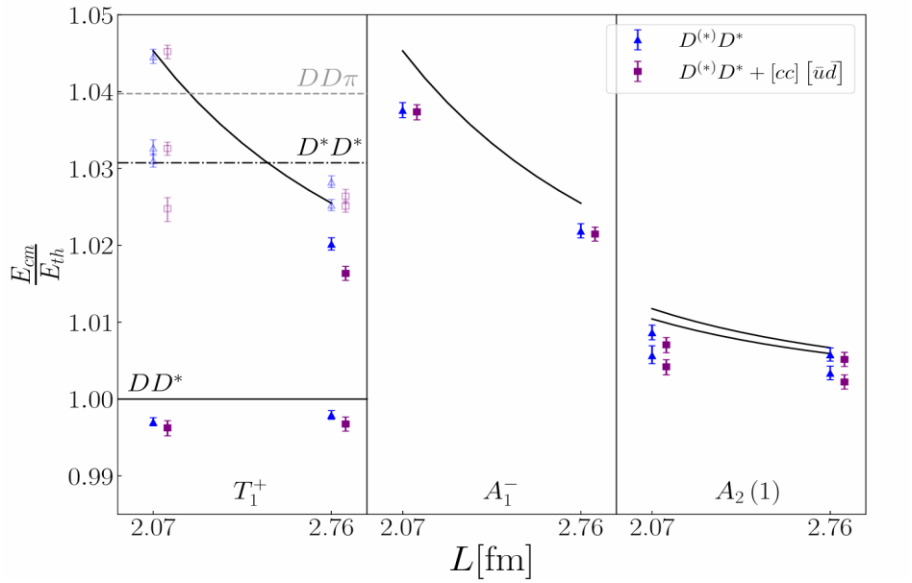


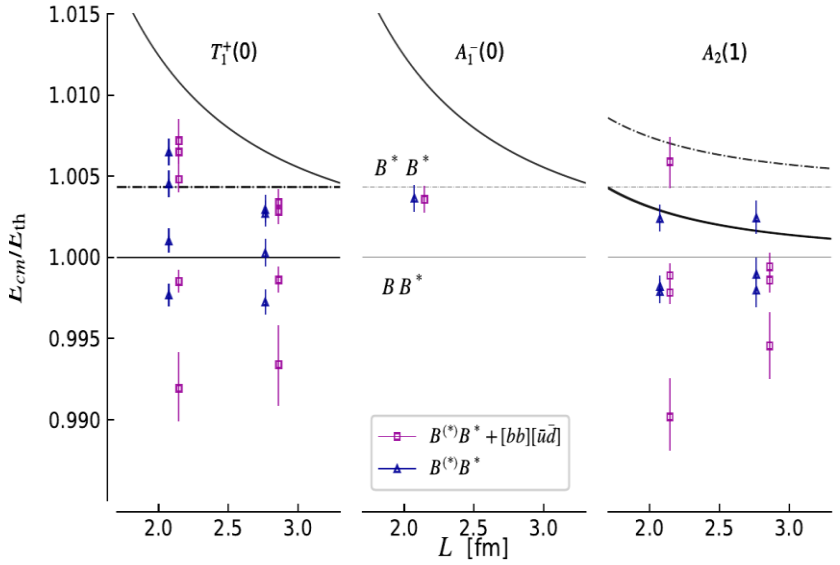
Cheung et al., JHEP 11 (2017) 033

V. Discussion on the relevance of local tetraquark operators

1. Doubly charmed and close-charmed tetraquark systems (T_{cc} and $X(3872)$)

- Experimentally, $T_{cc}^{+}(3875)$ and $X(3872)$ are very close in mass to the corresponding DD^* threshold.
- Theoretically, near-threshold pole singularities are derived for both cases.
- So the hadron-molecule interpretation seems more natural.
- As for the relevant of tetraquark operators——the completeness of operator sets.





Prelovsek et al., Phys. Rev. D 112, 014507 (2025)

V. Discussion on the relevance of local tetraquark operators

1. Doubly charmed and close-charmed tetraquark systems (T_{cc} and $X(3872)$)

- Experimentally, $T_{cc}^{+}(3875)$ and $X(3872)$ are very close in mass to the corresponding DD^{*} threshold.
- Theoretically, near-threshold pole singularities are derived for both cases.
- So the hadron-molecule interpretation seems more natural.
- As for the relevant of tetraquark operators——the completeness of operator sets.

- ✓ **Inclusion of $\mathcal{O}^{4q}$ operators does not add new energy levels (new states).**
- ✓ **Inclusion of $\mathcal{O}^{4q}$ may have effects on the determination of the finite volumes.**
- ✓ **Generally speaking, $\mathcal{O}^{4q}$ operators are usually linearly independent of meson-meson operators.**
- ✓ **Inclusion of $\mathcal{O}^{4q}$ makes the operator basis more complete (in some cases).**
- ✓ **Strictly speaking, the structure of operators do not necessarily reflect the internal structure of states.**
- ✓ **It is desired to find other probe to the internal structure of tetraquarks.**

2. T_{bb} state

- All the lattice QCD studies have consensus on the existence of a $0(1^+)$ bound state T_{bb}.
- The binding energy ranges from ~ 100 MeV to ~ 200 MeV. What is the physics behind this?
- The bound state mass is far from BB^* threshold, so it is difficult to interpret it to be a BB^* molecule.

- A $[bb][\bar{u}\bar{d}]$ tetraquark state? Seems supported by the charge distribution.

- Still an open question.

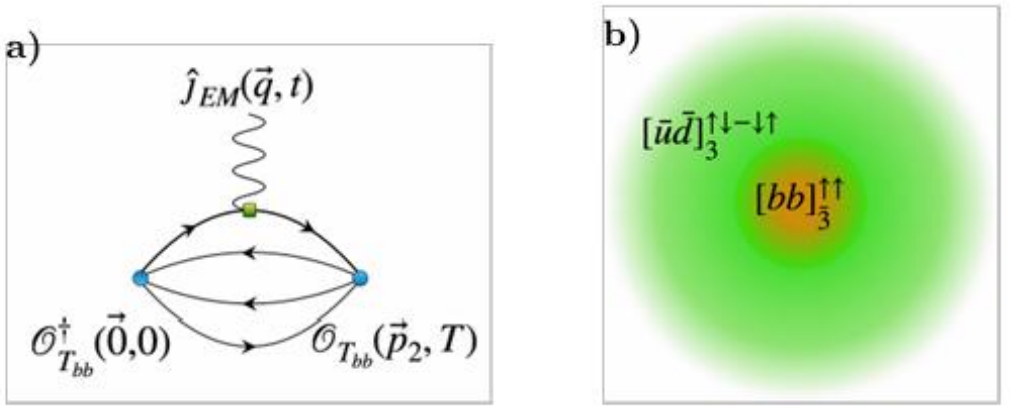


FIG. 1. **a)** Example of a connected Wick contraction diagram generated by the T_{bb} three-point correlator (6). **b)** Pictorial representation of the resulting distributions for light and heavy quarks.

S. Prelovsek, Phys. Rev. Lett. 136, 161901 (2026)

3. Fully charmed tetraquark systems

Experimental sector:

- CMS (Run-II and Run-III data) analysis determines $J^{PC} = 2^{++}$ quantum numbers of $X(6600), X(6900)$ and $X(7100)$ (CMS, Nature 648 (2025) 8092, 58-63).
- $X(6600), X(6900)$ and $X(7100)$ are sorted into a family of 2^{++} compact tetraquark states $[cc]_1^{3^*,S}[\bar{c}\bar{c}]_1^{3,S}(L = 0)$:

  The spin-1 diquark and anti-diquark can make 2^{++} state easily.
  While two charmonia (not necessarily spin-1) make 2^{++} less likely.

Lattice QCD calculation:

- A 2^{++} resonance is observed in $J/\psi J/\psi$ scattering and is consistent with $X(6600)$.
- The appearance of this resonance is associated with a CDD zero of the scattering amplitude.
- Sometimes, CDDs have connections with bare states (F.J. Dyson, Phys. Rev. 106, 157 (1957); M.I. Krivoruchenko et al., Phys. Rev. C 82, 018201 (2010); Y. Li et al., Phys. Rev. D 105, L071502 (2022))
- Phenomenolgocal studies predict the fully charmed tetraquark spectrum fully charmed tetraquarks (Q.-F. Luu et al., Eur. Phys. J. C 80, 871 (2020); G.J. Wang et al., Phys. Rev. D 104, 036016 (2021))

J^P	Configuration	$\langle H\rangle$ (MeV)	Mass (MeV)	Eigenvector
0^{++}	$\|\{cc\}_1^3\{\bar{c}\bar{c}\}_1^3\rangle_0$ $\|\{cc\}_0^6\{\bar{c}\bar{c}\}_0^6\rangle_0$	$\begin{pmatrix}6501 & -52\\ -52 & 6475\end{pmatrix}$	$\begin{bmatrix}6435\\ 6542\end{bmatrix}$	$\begin{bmatrix}(0.617, 0.787)\\ (0.787, -0.617)\end{bmatrix}$
1^{+-}	$\|\{cc\}_1^3\{\bar{c}\bar{c}\}_1^3\rangle_1$	6515	6515	1
2^{++}	$\|\{cc\}_1^3\{\bar{c}\bar{c}\}_1^3\rangle_2$	6543	6543	1
0^{++}	$\|\{bb\}_1^3\{\bar{b}\bar{b}\}_1^3\rangle_0$ $\|\{bb\}_0^6\{\bar{b}\bar{b}\}_0^6\rangle_0$	$\begin{pmatrix}19246 & 20\\ 20 & 19210\end{pmatrix}$	$\begin{bmatrix}19201\\ 19255\end{bmatrix}$	$\begin{bmatrix}(-0.410, 0.912)\\ (0.912, 0.410)\end{bmatrix}$
1^{+-}	$\|\{bb\}_1^3\{\bar{b}\bar{b}\}_1^3\rangle_1$	19251	19251	1
2^{++}	$\|\{bb\}_1^3\{\bar{b}\bar{b}\}_1^3\rangle_2$	19262	19262	1

Q.-F. Luu et al., Eur. Phys. J. C 80, 871 (2020);

0^{++}	Mass	$\bar{3}_c\otimes 3_c$	$6_c\otimes\bar{6}_c$	$1_c\otimes 1_c$	$8_c\otimes 8_c$	r_{12}/r_{34}	r	r_{13}/r_{24}	r'
1S	6405	31.9%	68.1%	96.9%	3.13%	0.52	0.31	0.48	0.37
	6498	67.7%	32.3%	5.7%	94.3%	0.51	0.36	0.51	0.36
2S	6867	10.6%	89.4%	80.6%	19.4%	0.65	0.35	0.58	0.46
	7007	89.7%	10.3%	26.0%	74.0%	0.49	0.47	0.59	0.35
1^{+-}	Mass	$\bar{3}_c\otimes 3_c$	$6_c\otimes\bar{6}_c$	$1_c\otimes 1_c$	$8_c\otimes 8_c$	r_{12}/r_{34}	r	r_{13}/r_{24}	r'
1S	6481	100%	0%	33.3%	66.7%	0.48	0.37	0.51	0.34
2S	6954	100%	0%	33.3%	66.7%	0.61	0.44	0.61	0.43
3S	7024	100%	0%	33.3%	66.7%	0.66	0.42	0.62	0.46
2^{++}	Mass	$\bar{3}_c\otimes 3_c$	$6_c\otimes\bar{6}_c$	$1_c\otimes 1_c$	$8_c\otimes 8_c$	r_{12}/r_{34}	r	r_{13}/r_{24}	r'
1S	6502	100%	0%	33.3%	66.7%	0.49	0.39	0.53	0.35
2S	6917	100%	0%	33.3%	66.7%	0.55	0.60	0.72	0.39
3S	7030	100%	0%	33.3%	66.7%	0.64	0.46	0.64	0.45

G.J. Wang et al., Phys. Rev. D 104, 036016 (2021)

VI. Summary

- Tetraquark states are investigated extensively and intensively by lattice QCD.
- Near-threshold structures are observed are relevant to T_{cc}, T_{bb} and $X(3872)$.
- There have no definite conclusions on the internal structures of these states.
- The properties of T_{bb} and $X(6600)$ hint at the possible existence of compact tetraquark degrees of freedom.

Thank you for your attention!

- **The above observation hints that the nucleon (and Roper) can be viewed as a two-body system of quark-diquark. However,**

$$\eta_2(\vec{x},t;\vec{r}) = \epsilon^{abc}[u^{aT}(\vec{x}+\vec{r},t)C\gamma_5 d^b(\vec{x},t)]\,u^c(\vec{x}-\vec{r},t)$$
$$\eta_3(\vec{x},t;\vec{r}) = \epsilon^{abc}[u^{aT}(\vec{x},t)C\gamma_5 d^b(\vec{x}+\vec{r},t)]\,u^c(\vec{x}-\vec{r},t)$$
$$\eta_4(\vec{x},t;\vec{r}) = \epsilon^{abc}[u^{aT}(\vec{x}+\vec{r},t)C\gamma_5 d^b(\vec{x}-\vec{r},t)]\,u^c(\vec{x},t)$$

Bethe-Salpeter wave function

$$\phi_n(r) \propto \langle\Omega|\eta(0,0;\vec{r})|n\rangle$$

The BS wave functions show that there is no obvious special correlations between any two quarks.

